Stratigraphy, Structure, and Mineralization of Kinsley Mountain, Elko County, Nevada

by

Bryan MacFarlane

A Thesis Presented in Partial Fulfillment
of the Requirements for the Degree
Master of Science

Approved March 2012 by the
Graduate Supervisory Committee:

Stephen Reynolds, Chair
Richard Hervig
Donald Burt

ARIZONA STATE UNIVERSITY

May 2012

ABSTRACT

The Kinsley Mountain gold deposit of northeastern Nevada, located ~70 km south of Wendover, Nevada, contains seven sediment-hosted, disseminated-gold deposits, in Cambrian limestones and shales. Mining ceased in 1999, with 138,000 ounces of gold mined at an average grade between 1.5-2.0 g/t. Resource estimates vary between 15,000 and 150,000 ounces of gold remaining in several mineralized pods.

Although exploration programs have been completed within the study area, the structural history and timing of precious-metal mineralization are still poorly understood. This study aims to better understand the relation between stratigraphy, structural setting, and style of gold mineralization. In order to accomplish these goals, geological mapping at a scale of 1:5,000 was conducted over the property as well as analysis of soil and rock chip samples for multi-element geochemistry.

Using cross-cutting relationships, the structural history of Kinsley Mountain has been determined. The deformation can broadly be categorized as an early stage of compressional tectonics including folding, attenuation of the stratigraphy, and thrust faulting. This early stage was followed by a series of extensional deformation events, the youngest of which is an ongoing process. The structural history determined from this study fits well into a regional context and when viewed in conjunction with the mineralization event, can be used to bracket the timing of gold mineralization. The northwest oriented structure responsible for concentrating decalcification, silicification, and mineralization has two generations of cave fill breccias that both pre- and post-date the gold event.

The statistical analysis of multi-element geochemistry for rock chip and soil samples has determined that Au is most strongly associated with Te, while weaker correlations exist between Au and Ag, As, Hg, Mo, Sb, Tl, and W. This suite of elements is associated with an intrusion driven system and is atypical of Carlin-type gold systems. From these elemental

associations the gold mineralization event is thought to be controlled by the emplacement of a felsic intrusion. The responsible intrusion may be an exposed quartz monzonite to the south of the study area, as suggested by possible zonation of Cu, Pb, and Zn, which decrease in concentration with increasing distance from the outcropping stock. Alternatively, an unexposed intrusion at depth cannot be ruled out as the driver of the mineralizing system.

ACKNOWLEDGMENTS

I would like to thank my advisors foremost for their patience while I completed this thesis. My family, especially my wife and newborn son for putting up with me while I compulsively overbooked my time commitments and then complained about it later. Without the people at Animas Resources, including John Wilson and Greg McKelvey, I would not have been able to complete this study. I appreciate and thank them for assistance with data collection, data analysis, field costs, and invaluable technical discussions. I thank my field assistant Adam Gorecki who kept me from going crazy in the sun of the Nevada desert, while I did my best to keep him out of the casinos. Consultants Odie Christensen, John Wilson, Chuck Thorman, Greg McKelvey, and Roger Steininger are especially thanked for challenging ideas and aiding in critical analysis of data as well as presenting alternative solutions. I would also like to thank Jeff Geier for editing this thesis, as well as detouring hundreds of miles out of the way from another property in Nevada to visit this field site "one more time".

TABLE OF CONTENTS

LIST OF FIGURES

Figure Page

Figure Page

LIST OF TABLES

Chapter 1

INTRODUCTION

General Overview

The Kinsley Mountain study area is located in northeastern Nevada, U.S.A (figure 1). The nearest city is West Wendover, Nevada, 68 kilometer (40 miles) north of the Kinsley Mine. Ely, Nevada, the next closest city, is 150 kilometers (92 miles) to the south. The mine, located within the Basin and Range physiographic province, is within the 12 km (7 mile) long, north-to-northeast-trending Kinsley Mountain. Kinsley Mountain is an offshoot

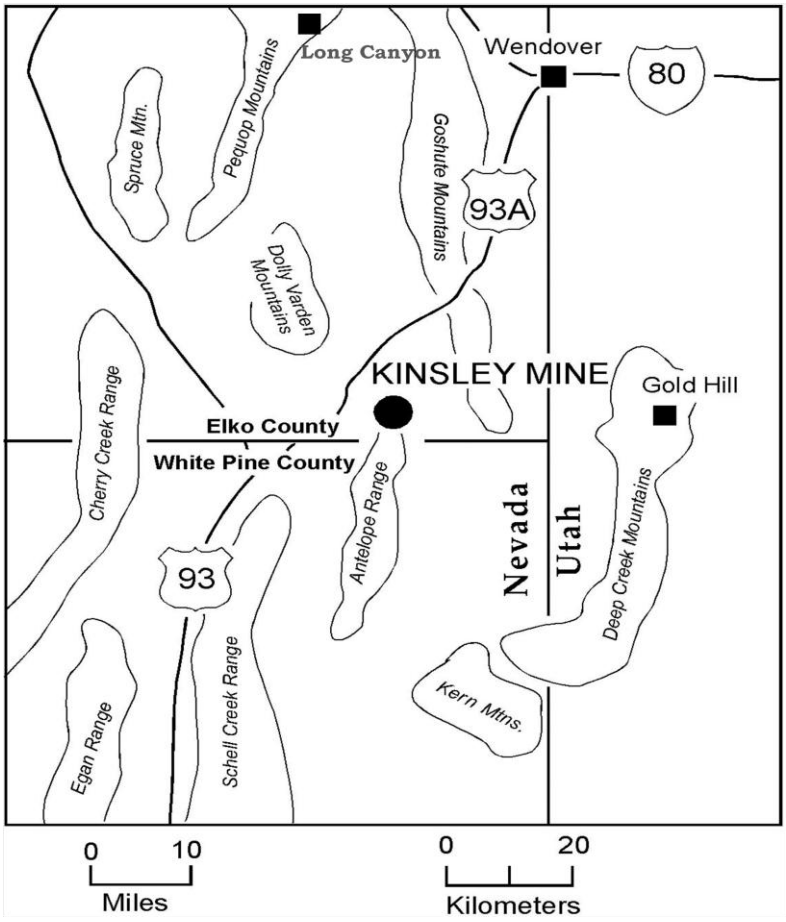

Figure 1. Map with the location of Kinsley Mountain, Long Canyon, and Gold Hill. (Modified from Robinson, 2005).

at the northern tip of the larger Antelope Range. The topography is moderately steep and locally rugged with a maximum elevation of 2400 m and local relief of 400 m. The mine can

be reached via highway 93A from either Wendover to the north or Ely from the south. Upon reaching the Kinsley Mine Road, which is a well-maintained dirt road, it is an additional 18 km drive to the mine. At the time of this thesis, the Kinsley Mountain study area consists of 141 unpatented load mining claims, as illustrated in figure 2.

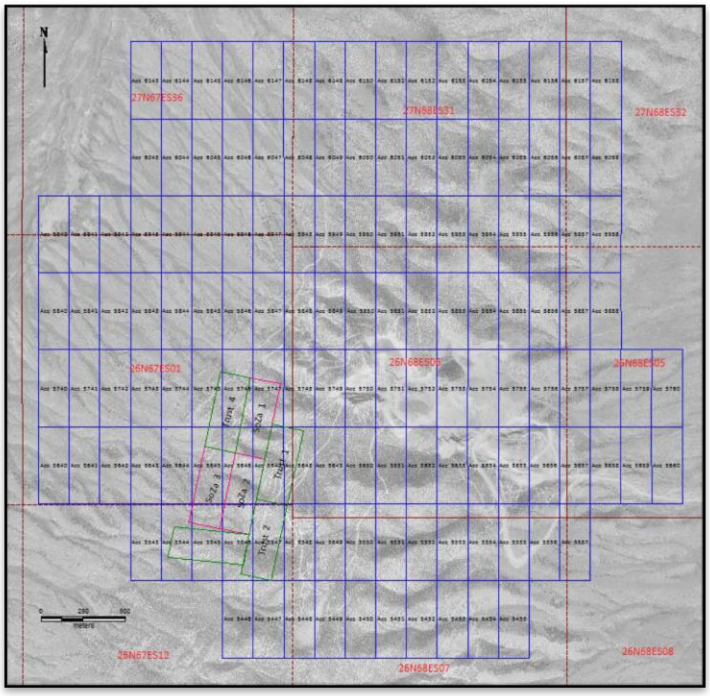

Figure 2. Map with the location of the 148 unpatented lode mining claims of the Kinsley Mountain Project. Claims are shown in blue rectangles, the Soza claims are shown as green and Pink rectangles.

The district is hosted in Cambrian to Ordovician, shallow-marine clastic and carbonate rocks of the Cordilleran miogeocline. Steininger (1966) and Buckley (1967) both noted carbonate rocks of Permian age in the southern tip of the range; however Cominco mapping (1982) grouped these units into the Cambrian section. Ordovician stratigraphy is represented by quartzite and dolostone. Bedding-parallel attenuation structures are present throughout the range, and like the stratigraphy, are folded in a regional-scale, gently northeast plunging, open to asymmetric anticline. The trend of the gently plunging fold approximates the trend of Kinsley Mountain. Exposed igneous rocks include a stock and

dikes of quartz monzonite to the south of the range and andesitic volcanic rocks surrounding the southern and western part of the range.

This study focused on understanding the stratigraphy, structure, and style of gold emplacement in the area surrounding the Kinsley Mine. The portion of Kinsley Mountain that has previously been shown to contain economic concentrations of gold mineralization is covered by 141 unpatented lode claims (figure 2). This area displays the most diverse alteration, style of deformation, and stratigraphic variation of the entire range. For these reasons, it is the best location to gain insight into the tectonic evolution of Kinsley Mountain. In this study, the area immediately south of the Kinsley Mine is an exposed stock of quartz monzonite with associated alteration. No geological mapping of the intrusion was conducted for this study, but the area was visited by the author on several occasions. The area to the north of the study area is composed of gently dipping carbonates of the Ordovician Pogonip Group.

The 11.5 km^2 study area is defined by the limits of the claims held by Nevada Sunrise Gold in their joint venture with Animas Resources, at the time of this writing. The black line on figure 3 represents the borders of this study and is coincident with the claim boundaries. Seven open pit mines are present within the study area along the northwest oriented structural zone. From southeast to northwest these pits are Access, Emancipation, Lower Main, Main, Upper Main, Upper, and Ridge (figure 4). In addition to mining over 135,000 ounces of gold, abundant exploration has been conducted including: geological mapping, geochemistry, geophysics, and drilling. Although some of the data were available to review for this study; the majority was not available. Many of the pits, including key observational points, have been partially backfilled, further complicating the interpretation process. Paper reports from previous companies were available for review.

Understanding the precious-metal mineralization along the Strip Fault, which cuts northwest across the center of the study area, and surrounding structural blocks was the

focus of this thesis. The goal is to define and place the known mineralization into a regional context, with the aim of applying this understanding to the search for similar deposits within the claim and remainder of the range. The primary tool used to accomplish this task was detailed geological mapping of rock type, alteration type, and structures. Additional support comes from soil, rock, and stream sediment geochemistry and statistical analysis of these data.

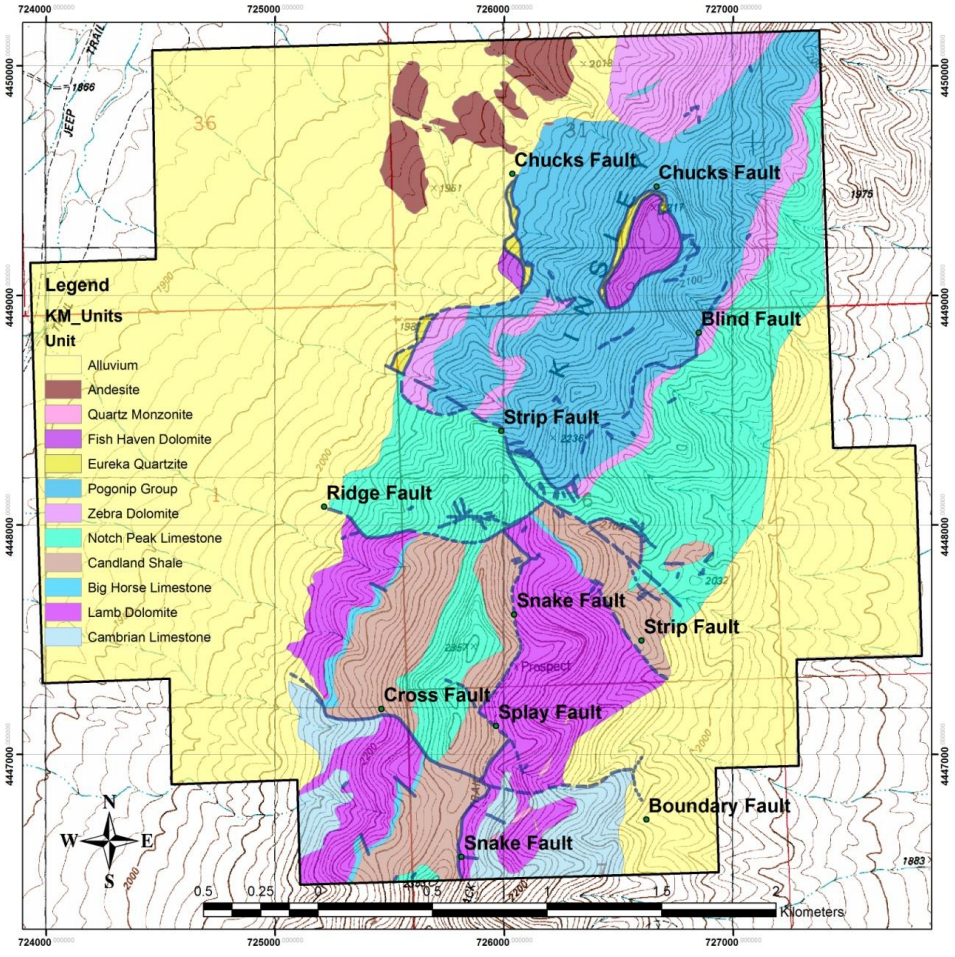

Figure 3. Geologic map of Kinsley Mountain showing the border of the study area and the names of significant structures. (MacFarlane, 2010).

Year	Gold	Silver	Copper	Lead	Tungsten
	lode, oz	ounces	pounds	pounds	units
1914	1	3560	11683	24343	
1915		186		19891	
1917	1	1142	2463	8701	
1919	1	106		4147	
1930	2	348	8577	3236	
1937	2	374	100	5400	
1940		63	1800		
1955		11	600		
1944-1956					127
Totals	**7**	**5790**	**25223**	**65718**	**127**

Table 1. Reported metal extracted from Kinsley Mountain between 1914-1956. (After LaPointe, 1991).

Previous Exploration and Mining Activity

Metal occurrences discovered within Kinsley Mountain include gold, silver, lead, copper, and tungsten (Hose et. al., 1976). Mining of these economic resources occurred in two phases. The first phase was focused on base-metal mineralization associated with contact metamorphism at the exposed contact between the quartz monzonite stock and undifferentiated Cambrian limestones. The second phase of mining was related to precious-metal mineralization, primarily gold. This mineralization occurs along a northwest trending structural zone (Strip Fault) that runs through the center of the study area (figure 3).

First Phase

Base-metal mineralization was first reported at Kinsley Mountain in 1862, as part of a prospecting study of the larger Antelope District (Cowdery, 2007; LaPointe, 1991). No mining activities occurred from the initial discovery, although areas with potential were prospected. It was 3 years later when George Kingsley in 1865 rediscovered this mineralization and regrouped several workings into the Kinsley District under the name of Kinsley Consolidated (Monroe, 1990). The properties under this consolidation were the

Phalen, Phalan-Keegan, Southam, Kerong, and Dunyon workings, which occur in both White Pine and Elko counties.

Mineral commodities, in order of decreasing extracted value, were copper, lead, silver, and tungsten, with lesser amounts of molybdenum, and gold (Monroe, 1990). Table 1 (reproduced after LaPointe, 1991), shows the production numbers of individual metals, as reported from 1914 through 1956.

LaPointe characterizes the mineralization as being associated with the quartz monzonite stock. Skarn, at the contact between quartz monzonite and sedimentary rocks, was most important to mineralization. This skarn grades into marble with increasing distance from the granitic rock. Schilling (1979), as referenced in LaPointe et. al. (1991) noted that a series of northeast-trending, quartz-latite porphyry dikes are associated with mineralization for at least 350m into the surrounding Cambrian limestones, with mineralization occurring on the margins of the dikes. Stager and Tingley (LaPointe et. al., 1991) document ore minerals present within the skarn to include molybdenite, chalcopyrite, galena, pyrite, scheelite, and powellite. They also mention the importance of proximity to the dike, which they classified as an alaskite. MacFarlane (2010) mentions a similar dike which outcrops approximately 200m from the mined strip.

Between May and September of 1963, seven inclined holes were drilled in the southern end of Kinsley Mountain. Accompanying this exploratory drilling, geologic mapping of the quartz monzonite and associated mineralization was carried out by Paige (1962). Since the completion of tungsten mining in the mid 1950's exploration at Kinsley Mountain has been focused on the precious metals gold and silver (Dunham, 1955; Quigley, 1966; Cowdery, 2007). Continued exploration led investigators away from the intrusive contact and further into the Paleozoic sedimentary rock package to the north, eventually resulting in a gold discovery.

Second Phase

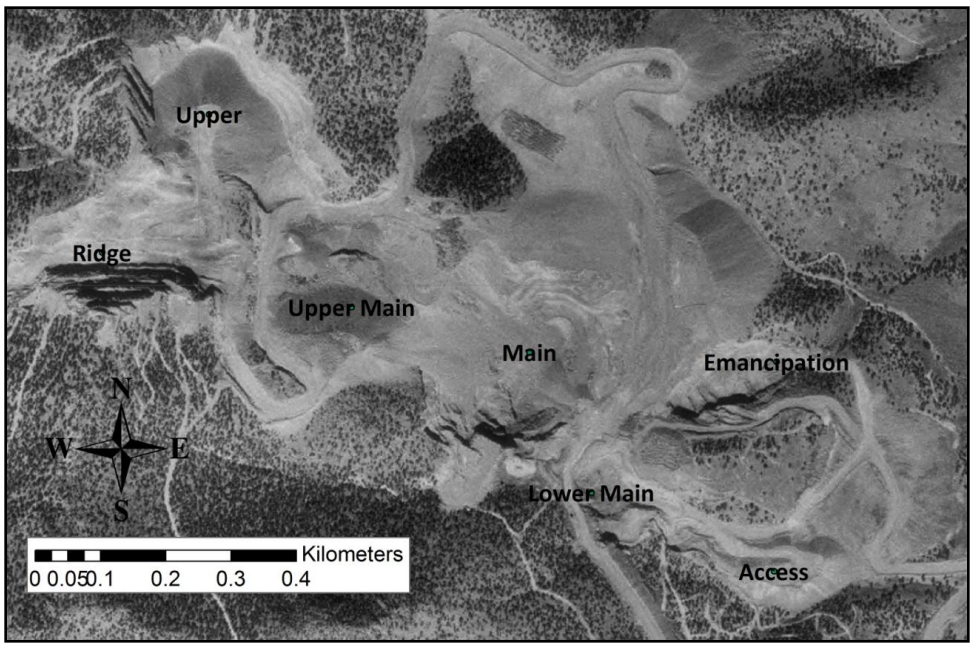

Figure 4. Black and white air photo with pit names. (US Department of Agriculture)

Precious-metal mineralization was discovered at Kinsley Mountain in 1984 by U.S. Minerals Exploration (Monroe, 1990). The discovery outcrop, in the area now known as the Main Zone (figure 4) was a large, gold-bearing jasperoid that contained 1.75 ppm gold in hand sample (Monroe, 1990). In January of 1985, U.S. Minerals Exploration entered into a joint venture agreement with Cominco American Resources Inc. Cominco follow-up rock samples at the discovery outcrop assayed up to 1 ppm gold (LaPointe, 1991; Monroe, 1990). By 1988, the joint venture announced 2.6 million tons of ore averaging 0.046 ounces per ton in the Main and Upper zones of the deposit (LaPointe, 1991). All of these 119,600 ounces of gold was cyanide-heap-leach-extractable oxidized ore.

According to Monroe (1990), the zone of gold mineralization, as defined by drilling, covers 7000 by 2000 feet. Gold mineralization is hosted in the Candland Shale, Windfall Limestone, Notch Peak Limestone, and to a lesser extent in the overlying limestones of the Pogonip Group. A total of seven deposits were eventually delineated along a northwest orientation, as shown in figure 4. This northwest orientation to the pits is further referred to

as the "mined strip". The individual deposits along the mined strip are the Main, Upper Main, Lower Main, Access, Ridge, Upper (a.k.a. Wod), and Emancipation, ordered by decreasing pit size. Four of the deposits were discovered within the first 67 holes drilled by Cominco. The Main deposit was discovered by the first drill hole, the Upper on the 21st drill hole, the Access was hit on the 40th drill hole, and the ridge zone was hit on the 48th drill hole (Monroe, 1990). These four deposits were all drilled in 1986, and were the largest of the deposits discovered along the mined strip (Christensen and MacFarlane, 2010). In total, more than 500 holes were drilled during the Cominco joint venture, but the project never made it to the production phase, while held by Cominco.

The Kinsley Property was optioned by Hecla Mining Company from Cominco in 1992. Hecla drilled 61 holes with 51 intersecting significant gold mineralization. Despite this successful drilling, the price of gold and high-start-up costs for a new project caused Hecla not to exercise their option agreement (Alta Gold, 1994). Meanwhile, Cominco decreased its land holding to the area immediately surrounding the drilled deposits. Some of the newly opened claims, along the western pediment, were immediately picked up by Rayrock, who were then taken over by Glamis Gold (Christensen and MacFarlane, 2010). Glamis Gold then drilled at least 4 drill holes, as well as running a 2-line resistivity and induced polarization survey (Steininger, 2010 pers. comm.). Some multi-element data are available for the drill holes, but gold is not included in the assay spreadsheets.

In 1993, Alta Gold negotiated a six month option-to-purchase-agreement with Cominco (Cowdery, 2003). In 1994, Alta Gold purchased the Kinsley Mountain property from Cominco, after a positive feasibility study by Kilborn Engineering Pacific (Christensen and MacFarlane, 2010). Included in this agreement was an option for Cominco/USMX to buy back part of the property should production exceed 300,000 ounces of gold (Alta Gold, 1994). An internal report from Alta Gold listed the following as positives for acquiring the

Kinsley property: it is a defined reserve, it is near Alta's production facilities, favorable metallurgy with a low strip ratio, ore is amenable to heap leaching, the property is on BLM land, and previous permits were on file. Mining began in 1995 and continued until 1999. Despite their predictions that total production from Kinsley would reach 200,000 ounces of gold, Alta Gold declared bankruptcy in 1999, reportedly due to expenditures at other projects. Along with mining, Alta Gold carried out an extensive exploration program with drill support. Despite these efforts, no additional large discoveries were made before bankruptcy was declared (Table 1). As Cowdery (2003) points out, Alta drilled in-fill holes around the pits and focused only on shallow oxidized ores that could be immediately transferred to the heap-leach facility for extraction.

Mining by Alta Gold produced 138,151 ounces of gold and 24,452 ounces of silver from the 7 pits shown in figure 4 (Christensen and MacFarlane, 2010). These pits, where economic mineralization was present, all occur along the mined strip. Table 2 shows the yearly production of both gold and silver between 1994 and 1999. Data for silver production were only available from 1995-1997.

KINSLEY PRODUCTION – ALTA GOLD		
Year	oz AU	oz AG
1994	0	*
1995	44,040	8,050
1996	44,553	10,930
1997	38,472	5,472
1998	9,543	*
1999	1,543	*
* = no value reported		
TOTAL oz	**138,151**	**24,452**
TOTAL tons of rock	193,411,400	978,080

Table 2. Gold and silver production from the mined strip. (Christensen and MacFarlane, 2010).

After the cessation of mining in 1998, no further production has been realized from Kinsley Mountain. This is not to say that exploration has ceased. After Alta Gold claimed bankruptcy, their claims were sold at auction. They were picked up by an auctioneer, who, according to Christensen and MacFarlane (2010), failed to cover the yearly property taxes. With this oversight, the claims became open and it was during this time that Nevada Sunrise Gold Corporation picked up the properties. Figure 3 shows the outline of the Nevada Sunrise claim block, which is coincident with the border of this study.

Nevada Sunrise hired geologist Jay Santos to conduct preliminary data collection and target generation. Mr. Santos contracted Calloway Exploration Services LLC to further delineate potential target areas. Calloway utilized a 30m digital elevation model of the mountain as a base layer upon which they overlaid Landsat images and available geochemical, structural, and alteration information in order to generate priority areas for further follow up work. Field checking of anomalies, as well as limited rock sampling, was conducted by Calloway. Santos followed up on the Calloway anomaly map by conducting his own limited rock-chip and soil-sampling survey. Santos also studied the deep refractory potential of the property based on the limited amount of deep drilling.

Animas Resources entered into a joint venture with Nevada Sunrise in 2010. Exploration conducted by Animas including geological mapping, geophysical surveys, and geochemical sampling. From these processes a new geologic model of mineralization was developed. Before drilling, Animas optioned the joint venture to Pilot Gold Corporation, who is currently in a joint venture agreement with Nevada Sunrise.

Up to the present, drilling has totaled at least 74,676 m (245,000 ft) in 1, 159 holes (Cowdery, 2007; Alta Gold, 1994; Steininger, 2010, pers. comm.). This drilling has identified a total of 17 target areas, including the 7 mined pits (figure 5). Cowdery (2007) determined

that 140,000 ounces of oxide ore may remain within these 17 targets, with an undefined amount of refractory ore which is also thought to be present. Santos

Organization	Year	Number of Holes	Footage	Av. Depth of Hole in feet
Cominco & Hecla	pre 1993	497	119,150	240
Alta Gold	1993	25	3,859	154
Alta Gold	1994	29	4,720	163
Alta Gold	1995	51	8,450	166
Alta Gold	1996	387	73,655	190
Alta Gold	1997	167	35,065	210
Alta Gold	1998	0	0	-
Totals		1156	244,899	212

Table 3. Table with drill holes at Kinsley Mountain separated by company, year, number, footage, and average depth.

(2007) however, estimates that only 14,572 ounces of oxide ore remain. The seven deposits mined by Alta Gold ultimately produced 138,151 ounces of gold (Table 3). Although the identified mineralization remaining in the ground may be too deep for economic production, more mineralization is present within Kinsley Mountain than has been extracted. In his 2007 technical report, Cowdery suggests that 140,000 ounces of already discovered gold is present within close proximity of the mined strip (table 4). As table 3 shows, the average depth of all drill holes is only 65 m (212 ft). Christensen and MacFarlane (2010) note that of the greater than 1,000 holes drilled, only a total of 31 have reached depths greater than 150 m (500 ft). Defining structural feeders and identifying non-outcropping prospective rock are future targets for precious metal exploration.

Name of Deposit	I.D. No.[1]	Alta Gold Est Size in sts.	Estimated range of sizes in sts.		Type of Mineralization
			Minimum	Maximum	
Emancipation	1	0[2]	0	50,000	Oxide
Lower Main	2	0[2]	0	5,000	"
Deep Main	3	150,000	0	200,000[3]	"
Access Extensions	4	3,000	0	10,000	"
Bojo	5	4,000	0	50,000[7]	"
Big Bend	6	220,000	50,000	300,000	"
Ridge Extensions	7	20,000[2]	0	50,000	"
Subtotal Main Zone areas		397,000	50,000	665,000	"
North Racetrack	8	20,000	10,000	50,000	"
West Racetrack	9	160,000	10,000	200,000	"
South Racetrack	10	0	20,000	50,000[4]	"
Baja Racetrack	11	100,000	10,000	200,000	"
Sub Total Racetrack areas		280,000	50,000	500,00	"
Wrong Spot	12	15,000	0	100,000[5]	"
Scorcher	13	20,000	10,000	100,000[6]	"
SoZa	14	0	5,000	150,000[8]	"
LBFJ	15	260,000	25,000	500,000[12]	"
Sub Total Misc. Oxides		295,000	40,000	850,000	"
Total of Oxide		972,000	140,000	2,015,000	"
139 Anomaly	16	126,000	0	N.E.	Carbonaceous Sulphides
SW Access	17	200,000[9]	0	N.E.	"
Total of Carbonaceous Sulphides		326,000	0[10]	9,900,000[11]	"

Table 4. Table with figures of expected gold mineralization, in ounces, at individual prospects and pits. After Cowdery, 2007.

The Kinsley Mountain gold deposit has been classified as a sediment-hosted disseminated gold deposit (LaPointe, 1991; Robinson, 2005). Gold mineralization occurs as bedding replacements and along steeply dipping structures. It is associated with silicification and areas of more intense structural preparation. Limestone was decalcified during the alteration process leaving a residual parallel to bedding. According to an Alta Gold internal report, a well developed footwall jasperoid was present along the mined strip. MacFarlane (2010) and Christensen and MacFarlane (2010) found that silicified cave fill sediments contained

elevated gold concentrations in the Ridge Pit, but that bedding-parallel shears, replacement, and decalcified limestone hosted mineralization in the Access Pit.

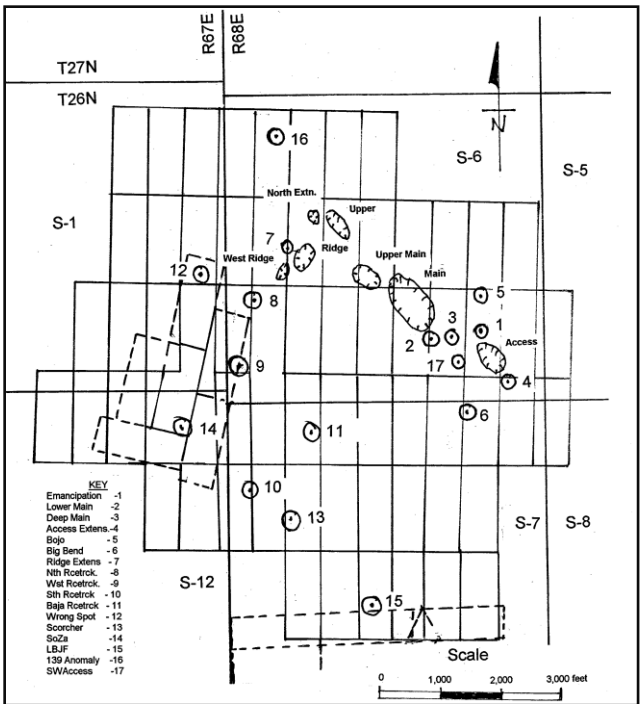

Figure 5. Map with labeled locations of all known gold anomalies within the study area. (Cowdery, 2003).

Previous Academic Studies

Three academic studies have been undertaken at Kinsley Mountain: Steininger (1966) from Brigham Young University, Buckley (1967) from San Jose State University, and DeSilets (1997) from the University of Nevada, Reno. Steininger focused on the characterization of the intrusive rocks of the Kinsley mining district. Buckley did not officially publish his results, but his focus was structure and stratigraphy of Kinsley Mountain. DeSilets was supported by Alta Gold during active mining, to conduct an ion pedogeochemistry survey.

The M.S. thesis by Steininger focused on the igneous rocks outcropping in the southern part of Kinsley Mountain. He noted several textures within the quartz monzonite intrusion, including a porphyritic phase. He also documented leucorhyolite and melanocratic

quartz monzonite dikes. Concerning the volcanic rocks, he determined three separate flows were present, all of which trend approximately N15W and are gently inclined to the east. Based on texture and composition, he classified the volcanic rocks as felsites rather than ignimbrites. Measurement of joints in the stock and country rock, dikes, and hydrothermal veins were plotted on rose diagrams by Steininger, from which a strong N30-40E trend was realized. Finally, he interpreted that the exposed stock was responsible for the dolomitization of the surrounding country rock.

Buckley, in his unpublished M.S. thesis, focused on the structural geology and stratigraphy of Kinsley Mountain. He is reported to have correlated the limestone above the shale unit to the Notch Peak Limestone of upper Cambrian age (Robinson, 2005). Buckley grouped rock types into Cambrian, Ordovician plus Silurian, and Permian units, rather than to separate them based on lithologies. His structural map also reveals that he interpreted the northwest-oriented mined strip to be at least two faults; one of unknown geometry and another as a low angle, extensional structure (figure 6) which places Ordovician and Silurian strata above Cambrian units (younger over older).

DeSilets used high-performance ion chromatography (HPIC) on soil samples collected by Cominco American between September 1985-1986. His association with Cominco provided him with abundant data, both geochemical and related to the ongoing exploration mapping. He attempted to use ion pedogeochemistry as a vector to identify unknown mineralization. The culmination of his thesis was a series of gridded plots for F^-, Cl^-, NO_2^-, Br^-, NO_3^-, PO_4^{3-}, SO_4^{2-}, AsO_4^{3-}, Li^+, Na^+, NH_4^+, and K^+. Based on his research, he concluded that two trends were present; a northwest-southeast trend that correlated to the mined strip and a less intense northeast-southwest trend that correlated to known alteration. He also determined both Pearson and Spearman correlation matrixes for all cations and anions studied. The correlations of the ions with gold was rather poor; in the

Pearson matrix there was no correlation, while in the Spearman matrix gold had a 0.2 correlation score with Cl^-, NO_2^-, and NH_4^+.

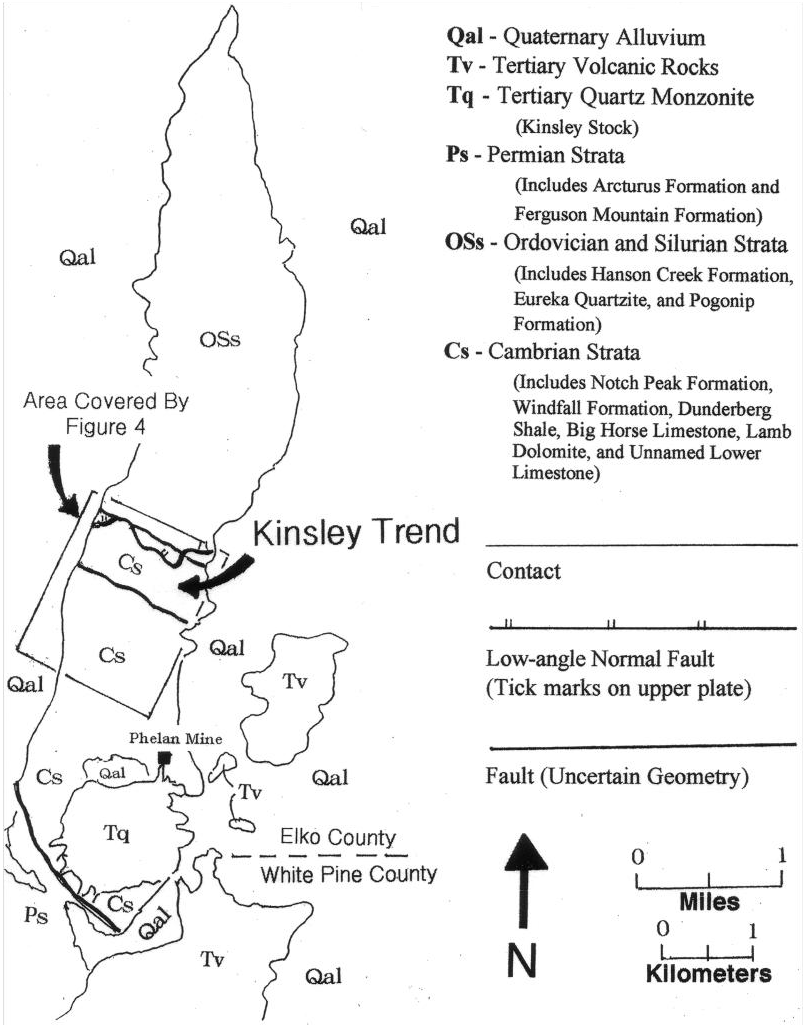

Figure 6. Structure and lithology map of Buckley (1967) with contacts between Tertiary, Permian, Ordovician, and Cambrian units shown. (modified by Robinson, 2005).

Chapter 2

ROCK UNITS

Regional Geology

Sedimentary rocks and deposits of northeast Nevada and western Utah range in age from Archean to Quaternary. Volumetrically, the largest percentage of these rocks are miogeoclinal sediments, recording 500 MY between the Neoproterozoic and the end of the Paleozoic era. Igneous rocks span around 200 MY of geologic time, with Jurassic to Miocene rocks being present. The youngest unit besides active basin fill is Pleistocene lacustrine sediments of Lake Bonneville.

The oldest documented rocks in northeastern Nevada are located in the East Humbolt Range and Ruby Mountains, where U-Pb geochronology has determined a minimum age of 2520±110 Ma in an orthogneiss exposed in the core of a nappe fold (Lush, 1988). Knowledge of the age of the oldest rocks present is critical to determining the age of the underlying basement. Utilizing the aforementioned radiometrically determined age, this region is underlain by rocks are part of the Archean Wyoming province. Premo (2008) asserts that inheritance of Proterozoic to Archean zircons occurred during a Cretaceous magmatic event in the Humbolt Range. His argument pushes the Cheyenne Belt, which is the boundary between Archean rocks to the northwest from Proterozoic rocks to the southeast, further north. Nelson (2011) places the Cheyenne Belt north of the Humbolt Range, but south of the Snake River Plain. Nelson further states that no Mojave terrain exists outside of the Mojave Desert region, thus inferring that the basement of northeastern Nevada actually belongs to the Yavapai province. Neoproterozoic rocks belonging to the Neoproterozoic McCoy Creek Group, Prospect Mountain Quartzite, and Busby Group, are exposed in the nearby Deep Creek and Pilot ranges. Perry (2010), utilizing detrital zircon geochronology, found age groupings at 1.0-1.2 Ga, ~1.4 Ga, and 1.6-1.8 Ga in the McCoy

Creek Group. She also used sedimentary features to determine local derivation of these sedimentary rocks. With a lack of zircons in the 2.0 Ga or older range and her interpretation that these clastic rocks were locally derived, it appears that the Neoproterozoic rocks of the Deep Creek and Pilot Ranges suggest a Yavapai basement underlies this part of northeast Nevada and northwest Utah.

Miogeoclinal sedimentary rocks of northeastern Nevada and northwestern Utah range in age from Neoproterozoic to Triassic in age. These rocks are dominated by carbonate lithologies, but clastic rocks, especially in the Precambrian and lower Cambrian parts of the section, are also present. Throughout the Cambrian, northeastern Nevada and western Utah were the edge of the continental platform (Hintze, 1988). Carbonate deposition was nearly continuous, with ratchety transgressions and erosional regressions occurring through the end of the Ordovician.

Mesozoic supracrustal rocks are not preserved in northeast Nevada, in part because of events after the transition from a passive to an active continental margin. During the Jurassic and Cretaceous periods compressional tectonic events created a series of fold and thrust belts that resulted in highlands in northeast Nevada and western Utah (DeCelles, 2004). Several workers interpret these mountains to be comparable to the modern Andean plateau, before extension. Debris eroded from the Nevada highlands were shed eastward into the foreland basin located in modern-day west-central Utah.

During the Tertiary, following the cessation of compressional tectonics, northeastern Nevada and western Utah began to extend under gravitational forces. The collapse of the previously elevated terrains produced large-scale basins. These basins are still actively opening and in-filling with material shed from the uplifted blocks. The filling of the basins involves both erosion of the surrounding ranges and extrusive volcanism of

intermediate composition. The thickness of the basin fill can range from a thin veneer to more than 3,000 m (10,000 ft.).

Sedimentary rocks in the areas surrounding Kinsley Mountain are Paleozoic carbonate and clastic materials deposited on the edge of the continental shelf and are part of the Carbonate Shelf Sequence of Nevada (Crafford, 2007). Hintze (1988) shows that quartz sands were being deposited regionally in the Early Cambrian. By Middle to Late Cambrian, shallow-marine limestone deposition would be widespread. According to Hintze (1988), shallow-water limestone deposition was continuous through the Late Ordovician with only thin, but widespread deposition of deep-water shales (figure 7). Figure 7 shows the cumulative thickness of Cambrian and Ordovician units in northwest Utah. Kinsley Mountain (KM) is just off these maps in the northern Utah Basin.

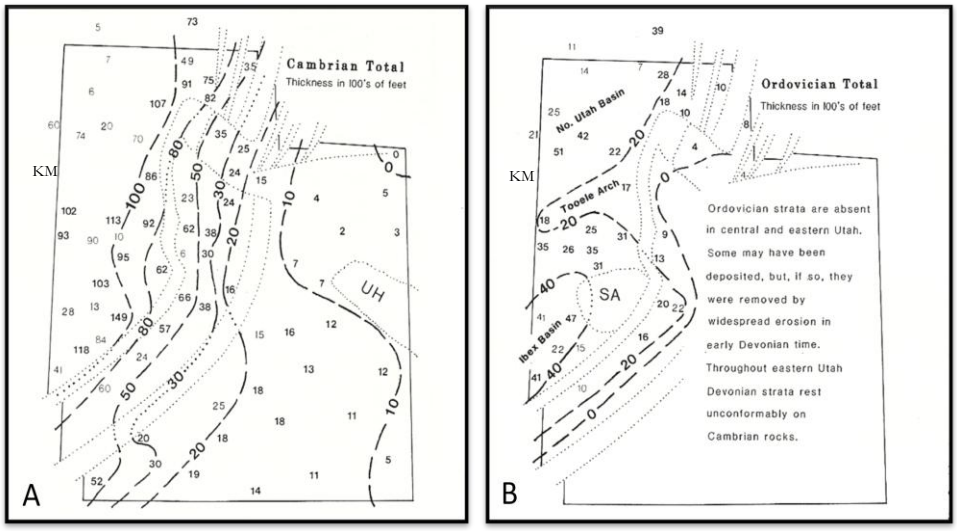

Figure **7**. Maps illustrating the extent and thickness of Cambrian (A) and Ordovician (B) units in Utah. From Hintze, 1988.

Intrusive rocks of northeast Nevada are typically granodiorite to monzogranite in composition (figure 8). Extrusive rocks range from basaltic to rhyolitic in composition. Geochronologic data of igneous rocks in northern Nevada reveals three pulses of increased thermal activity (DuBray, 2007; Miller et. al., 1987). Three major pulses of igneous activity

occurred during the Jurassic (175-145 Ma), Cretaceous (115-65 Ma), and Mid-Tertiary (40-15 Ma), respectively (figure 9).

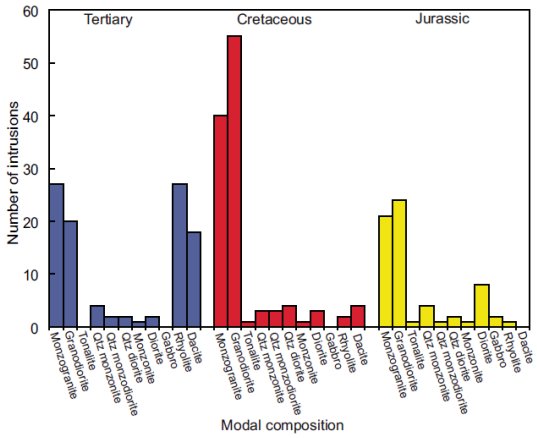

Figure 8. Frequency and modal composition plot of intrusive events through geologic time in Nevada. After DuBray, 2007.

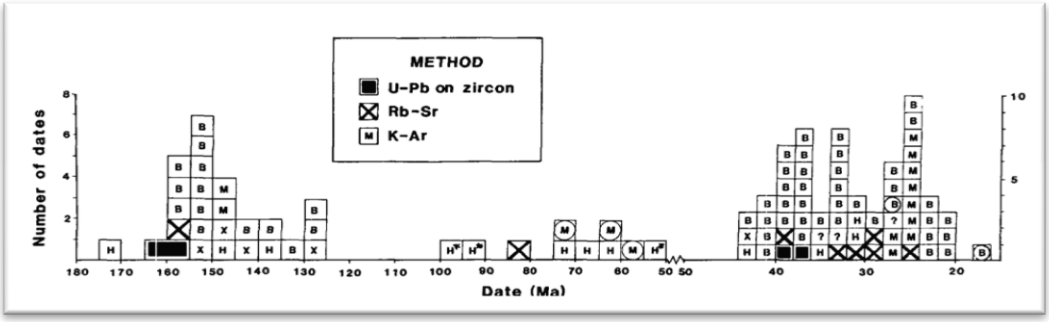

Figure 9. Geochronology of intrusive rocks of northeastern Nevada. Miller et. al. 1987.

Jurassic intrusive rocks formed in a backarc setting, related to the opening of a slab window (DuBray, 2007). Jurassic plutons can be associated with large, thermal alteration zones including base-metal mineralization, as observed in several of the surrounding ranges (Miller, 1987). Cretaceous magmatism was produced during the flattening of the subduction angle of the down-going slab and the resulting landward sweep of the magmatic front (DuBray, 2007; DeCelles, 2004). Tertiary bi-modal volcanism is associated with post-collisional extension and rifting of the Basin and Range province.

Mesozoic intrusive rocks are regionally important due to their temporal relation to structures and mineralization. The thermal event outlasted synchronous contractile deformation and allows for the separation of Mesozoic orogenic events. These granitic rocks both pre- and post-date the development of regional fabrics (Thorman, 2010 pers. comm.).

Mid-Tertiary igneous activity occurred during the interval 40-15 Ma. This event is associated with intermediate volcanism, with andesitic vents and flows present throughout the surrounding basins. The youngest of these volcanic rocks are typically of rhyolite-dacite in composition (DuBray, 2007).

Igneous rocks of the Jurassic, Cretaceous, and Tertiary periods are known to be present in the ranges immediately surrounding Kinsley Mountain. In the Goshute-Toano Range, structural levels reveal differing intensities of intrusive activity, with rocks of the lower plate undergoing a more intense thermal history than rocks of the middle block. The highest structural levels reveal little evidence of the complex history of intrusion. In the Dolly Varden Mountains, to the west of Kinsley Mountain, the Melrose Stock, a Mesozoic quartz monzonite has been radiometrically determined to be 165-134 Ma (Zamudio and Atkinson, 1992). This quartz monzonite is associated with copper and gold mineralization in the Dolly Varden Mountains. In the Deep Creek Range, to the east of Kinsley Mountain, the Ibapah Pluton has been determined to be 39 Ma (Rodgers, 1989). This pluton intrudes into a west-northwest structure. At Kinsley Mountain, the quartz monzonite stock at the south of the mountain has been radiometrically determined to be 34Ma (Maldonado et. al., 1988)

The stratigraphic framework of northeast Nevada and western Utah has been complicated by several episodes of both compressional and extensional tectonics. To further complicate the stratigraphy, syn-depositional Paleozoic flexure of the continental margin has been proposed (Hintze, 1988) to explain local thinning of units (figure 7B).

However, Welsh (1994) points out that Paleozoic arches were commonly accepted before 1940. Later work showed that tectonic attenuation is responsible for the thinning and complete removal of stratigraphy, both as extensional and compressional structures. The most recent studies (Welsh, 1994; Ketner et. al., 1998; Nutt and Thorman, 1994) conclude that Mesozoic contractional deformation is responsible for the observed attenuation of units. Chuck Thorman, in a field visit to Kinsley Mountain in 2010, was of the opinion that "the units are attenuated by younger over older thrust system" at Kinsley Mountain. Furthermore this deformation was a result of contractional deformation, potentially associated with the Middle Jurassic Elko orogeny, Late Cretaceous to Early Cenozoic Sevier orogeny (Thorman, 2010).

Kinsley Mountain General Lithology

The rock types of Kinsley Mountain are composed of carbonate and clastic rocks of Cambrian through Ordovician age. These carbonate and clastic rocks represent miogeoclinal sediments that were deposited along the continental shelf from the Cambrian through the Triassic in northeastern Nevada (Hintze, 1988). The oldest unit outcropping within the Kinsley Range is a Cambrian limestone. Robinson (2005) proposed that the lower limestone may correlate to the Abercrombie Formation, which is present in a similar stratigraphic horizon at Gold Hill, 40 km to the east in the Deep Creek Range. The youngest sedimentary rocks exposed in the Kinsley Range are dolostones of Ordovician age, which occur in the hangingwall of an attenuation structure placing younger over older units. Permian sedimentary rocks have been documented by Steininger (1966) and Buckley (1967), as well as on the Nevada Bureau of Mines and Geology: geological map of Nevada (Crafford, 2007).

Sedimentary Sequence

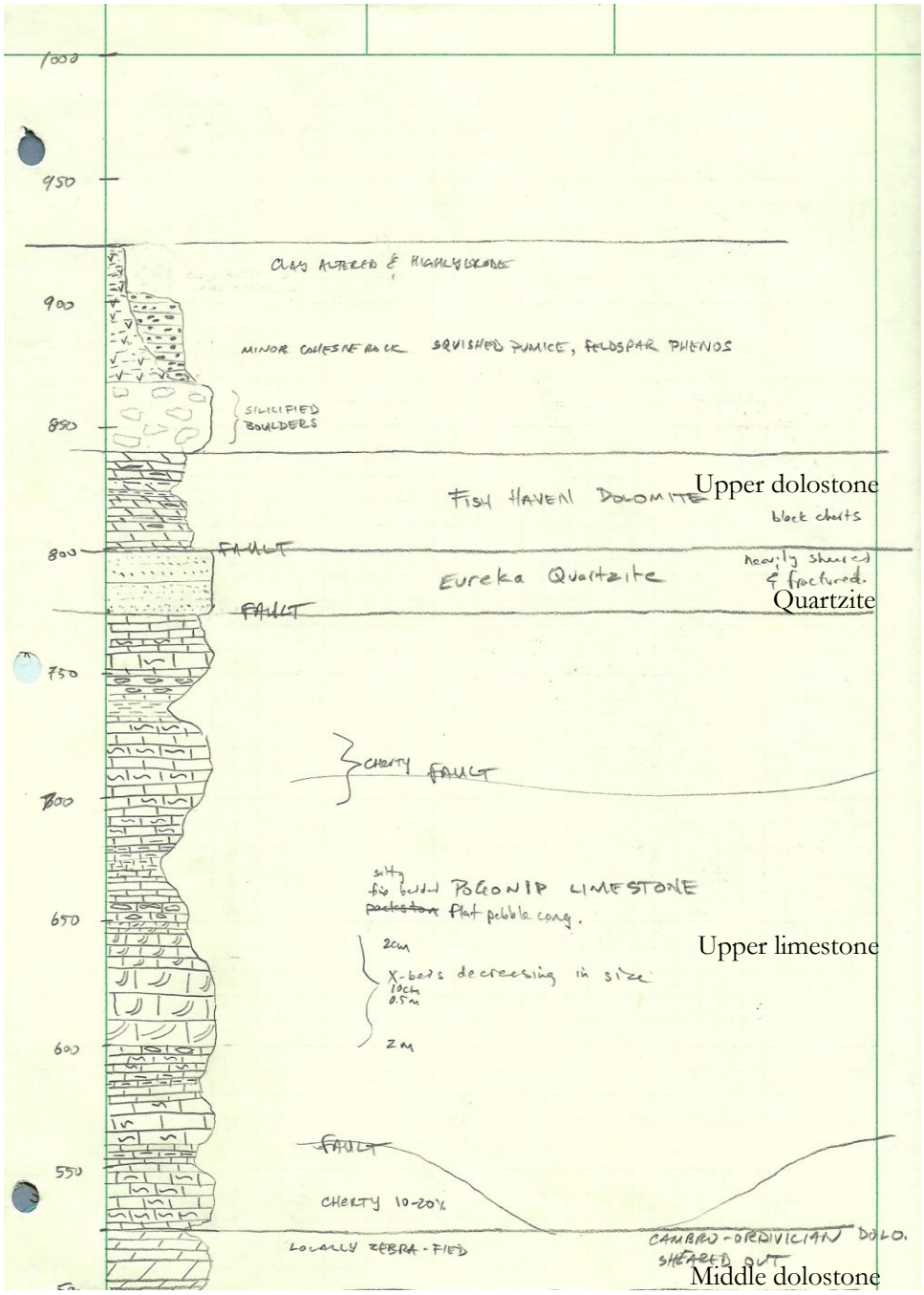

Figure 10. Kinsley Mountain stratigraphic column. Units are meters (MacFarlane, 2010).

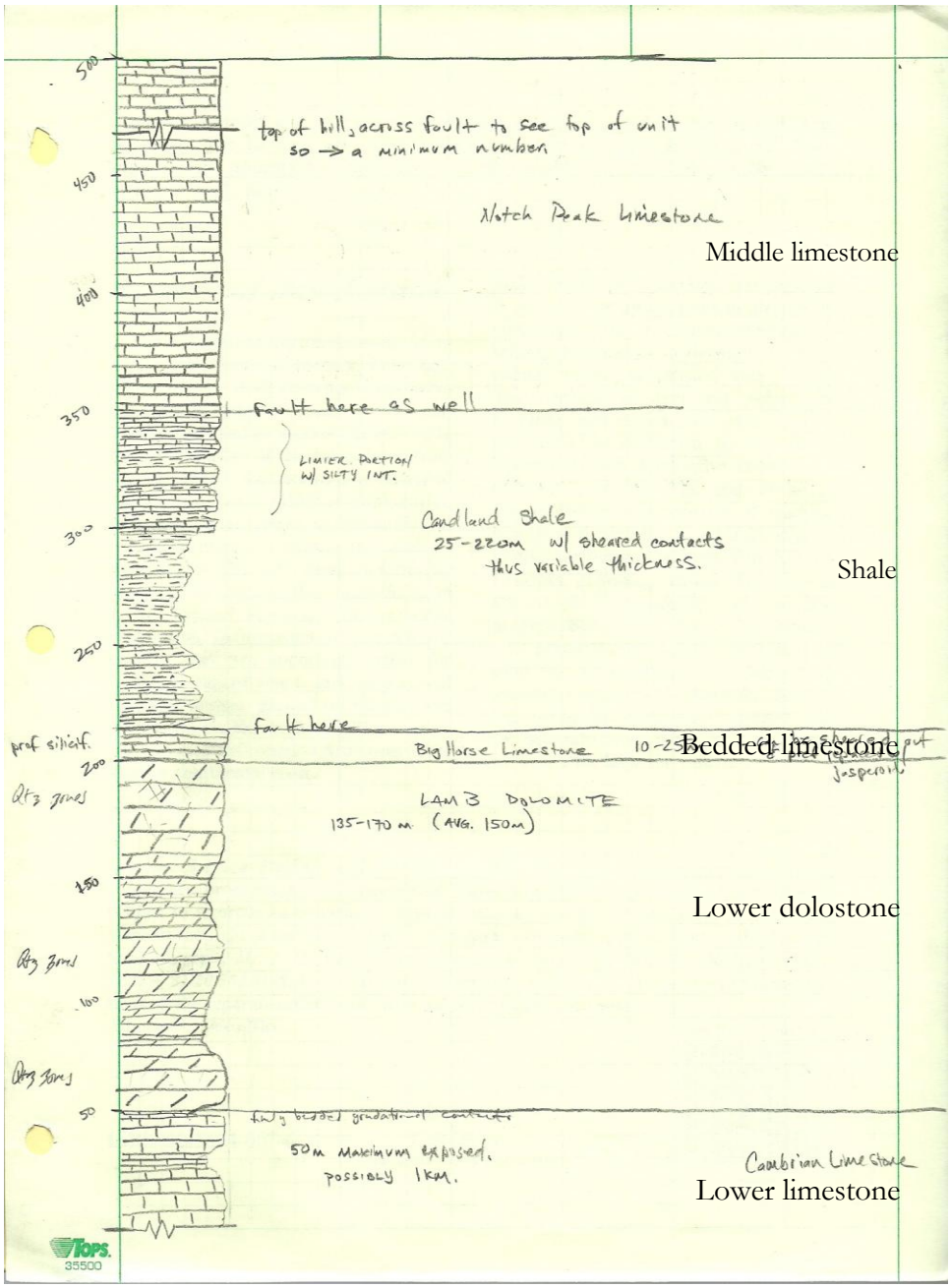

Figure 11. Continuation of Kinsley Mountain stratigraphic column. Units are meters (MacFarlane, 2010).

Lower limestone

The lower limestone is a massive, medium-grained, fetid, gray to dark gray limestone with fossil hash (0-10%) and chert stringers (0-25%) parallel to bedding. Bedding thickness

ranges from 5 cm to 1 m with great variation. Local siltstone interbeds are present with no apparent lateral continuity. The upper contact is transitional with the overlying dolostone, with limestone beds thinning and picking up a darker color over five meters as the contact is approached. The upper contact is best exposed along ridges on the east side of the range, near the quartz monzonite dike. The lower contact is nowhere exposed in the Kinsley Range but regionally correlative units can reach thicknesses in excess of one kilometer. From cross sections, the maximum thickness exposed was determined to be less than 50m, but the unit covers large areas due to gentle folding and to dip faces that dip approximately parallel to the steepness of the slope (figure 3; figure 18).

Lower dolostone

The lower dolostone unit is a cliff-forming dark gray, medium-to-coarse-grained, fetid, sugary textured, dolostone with local fossil hash (up to 40%). Black chert stringers, nodules, oolites, and stromatolites have been observed (MacFarlane, 2010; Robinson, 2005). Both the lower and upper contacts have been observed to be gradational, although they can be faulted as well. The upper contact can localize shearing due to contrasting rock strengths between dolostone and bedded limestone with shale. Individual dolostone beds range from 10-50 cm, but can also be massive, with the orientation of bedding difficult to determine. Quartz veins are common within this unit, occurring as veins, swarms, and fracture fill.

Bedded limestone

The bedded limestone unit is a thinly bedded, dirty, gray limestone with variable thickness and a wavy texture. The unit can be sheared, with thickness variations ranging from not present to a maximum of 5 meters thick (Figure 18). This unit is a transition between the lower dolomite and shale and is preferentially converted to a bedding replacement, non-destructive jasperoid. Primary textures are preserved where later shearing has not overprinted them. Individual beds are 1-3 cm thick with local shale interbeds less

than 1 cm thick. Both the upper and lower contacts are thought to have originally been conformable, but are sheared where best exposed.

Shale

The shale unit is a finely bedded, moderately to strongly fissile siltstone that ranges from weakly to strongly calcareous with interbeds of medium-to-dark-gray and black limestone 2 cm-1 m wide. The shale is olive green to dark gray when fresh, but weathers to a brownish tan color that can get a red stain where sulfides are oxidized, The shale can display a weak to strong (in comparison to bedding) cleavage at low to moderate angles to bedding. The shale preferentially weathers, forming gentle slopes with no exposure except the local rib of limestone. In areas of bedding-parallel shearing, boudins of both limestone and dolostone have been observed to "float" within the shale beds. Both the upper and lower contacts are thought to originally have been gradational, as limestone content increases when they are approached. Both contacts also focused deformation as evidence by faults exposed in the pits.

Middle limestone

The middle limestone unit is a bedded, black limestone with fossil hash (up to 50%), black chert nodules. In the mined area, a pink bedding-parallel residuum is commonly developed as a result of decalcification. Whole trilobites have been observed, as well as abundant fossil fragments. Dolostone interbeds were observed from the base of the section to the top of the section, but contribute little to stratigraphic thickness of the unit. Several sub-units exist within the middle limestone, including a basal fine to massively bedded limestone grading into laminar-to-burrowed limestone, grading into medium to coarse-bedded cherty limestone. Individual beds range from less than 1 cm to greater than 10 cm with pink bedding-parallel residuum 1 mm-1 cm wide. The amount of bedding parallel residuum present decreases away from the mined strip. The lower contact is gradational with the underlying shale, but is faulted where exposed in Main Pit. The upper contact is

not clearly exposed south of the mined strip. North of the mine, across a structurally complex zone, the upper contact is gradational into a dolostone unit, but can also be in fault contact with the overlying upper limestone (Figure 3).

Middle dolostone

The middle dolostone unit is a banded, white and dark-gray to moderately dark-gray, coarse-grained dolostone with local chert stringers parallel to bedding (up to 50% volume). The banding is an alteration product, as it ranges in intensity and can be non-existent. The composition of the white bands can be white dolomite, quartz, or less commonly calcite. Individual beds range in thickness from thin to massive. Both the lower and upper contacts are gradational, although the upper contact can be sheared out by a low-angle structure.

Upper limestone

The upper limestone unit is a primarily gray, medium-grained, fine-to-thick bedded, fossiliferous limestone with bedding parallel chert stringers (up to 50% volume). Dolostone intervals are present and most common on the west slopes, north of the mined strip. Individual beds of both limestone and dolostone range from 1 mm-25 cm and consist primarily of bedded limestone. Flat-pebble conglomerates, cross-bedded carbonate sands and fining-upwards sequences of carbonate sands and muds are also present. The group could be further subdivided, because zones of dolostone, variably intense chert, finer and coarser bedding, and dirty to pure limestone exist with map-scale thickness. The lower contact is gradational from the middle dolostone, but a series of low-angle and bedding-parallel structures cut this unit with unknown stratigraphic implications. In the mine area, the upper limestone is separated from the middle limestone by a low-angle structure. A major unconformity exists at the upper contact where up to 1 km of sediments could be missing between the Pogonip Group and Eureka Quartzite (Thorman, 2010).

Quartzite

The quartzite unit is a pure-white, massively bedded quartzite that is resistive to weathering and forms prominent cliffs. On the northwestern side of the range, quartzite clasts dominate the alluvium and sediments in the drainages. The quartzite roughly defines the contact with the colluvium and alluvium northwest of the mined strip. The quartzite unit best defines the regional fold, with bedding measurements ranging from horizontal on the ridge top to vertical on the west slope (figure 18). The lower contact is faulted where exposed, with complete removal of the unit in the ridge-top klippe (figure 3).

Upper dolostone

The upper dolostone unit is a dark gray to black dolostone with black chert stringers parallel to bedding. Individual beds range from 2-10 cm. The lower contact is a bedding parallel structure that can remove the underlying quartzite, resulting in upper dolostone in contact with upper limestone. The lower contact may have originally been gradational as interbeds of sandy black dolostone and clean, cross bedded, non-calcareous, white quartzite alternate, grading upwards into pure dolostone. The upper contact is nowhere exposed in the range. Similar to the underlying quartzite, bedding measurements in this unit show it to be horizontal at higher elevations and vertical at the western alluvium to bedrock contact.

Igneous Rocks

Intrusive Rock

The stock and dike of intrusive rock is a tan to brown quartz monzonite with a strike length of 2 km. This dike has been traced from the southern border of the study area to 400 meters from the mined strip. It strikes northeast with variable thickness between 2-15 m. It is composed of 50% phenocrysts and 50% matrix. Coarse crystals consist of white to pink feldspar (40%), clear feldspar (30%), biotite (25%), and quartz (4%) on average. It is also weakly magnetic (<1% magnetite) and can be highly calcareous where in contact with limestone. Contact metamorphism with chill margins less than 25 cm into the monzonite

and 30 cm of limestone recrystallized to marble are present. Locally, skarn of magnetite and yellowish-green garnet are developed in minor amounts. The dike is visually similar to the larger stock exposed at the south end of the range. It has been observed to cut stratigraphy through the lower dolostone unit in outcrop, but pieces (not in place) have been observed in waste material of the Access Pit entrance road (figure 4). This suggests that the dike may intrude the stratigraphy as high as the shale unit and may project north at least to the Strip Fault. According to Monroe (1990), "dikes are commonly encountered in holes drilled near the range front (east side)". Robinson (2003) also adds "It was also noted that a number of volcanic intrusions occur along the base of the range, on both sides and to the north and south (of the mine)".

Extrusive Rock

The extrusive rocks present are a maroon, finely crystalline andesitic tuff with pumice and a basal silica breccia. The andesite tuff has a fine matrix but can have white feldspar phenocrysts up to 3 mm, biotite crystals up to 3 mm, and both pumice and lapilli. The andesite is strongly altered to clay by weathering. Where solid outcrop exists, a compaction foliation strikes roughly north-south and gently dips to the west, similar to the steepness of the western slope of Kinsley Mountain (figure 3). To the south of the range, an andesitic flow with autoclastic brecciation was observed to be cut by dikes of similar composition. Large volumes of andesite tuff blanket the low lying carbonate hills in the basins surrounding Kinsley Mountain.

Colluvium and Alluvium

The colluvium and alluvium consist of an angular assortment of clasts containing all lithologies present within the range. The colluvium can be used to map the subsurface as contacts show up as mixtures of fragment types near the contact, grading into homogenous compositions away from contacts. This suggests that the colluvium on the slopes is a thin

veneer. The colluvium grades into alluvium towards the basin. Gravels associated with active drainages overlie the andesite, but older alluvium likely underlies the andesite.

Discussion of Rock Types

Figure 12 illustrates the interpretation of stratigraphic correlations for the mapped units of Kinsley Mountain. It must be noted that fossil correlation was not undertaken and that correlations are strictly based on descriptions of stratigraphic sections given by other authors (Nutt, 1994; Hintze, 1988). Figure 7 (Hintze, 1988) shows the thicknesses of Cambrian-Ordovician rocks in Utah. From this information, approximations of the paleo-shoreline and expected lateral trend of units can be made. Following this reasoning and due to the close proximity of Kinsley Mountain to the Utah border (30 km /20 miles), the Utah stratigraphic packages can be projected to Kinsley Mountain.

The stratigraphic correlations made from review of stratigraphic sections and comparison with the stratigraphic column from Kinsley Mountain is shown in table 4. The correlations are also shown on the stratigraphic column (table 4).

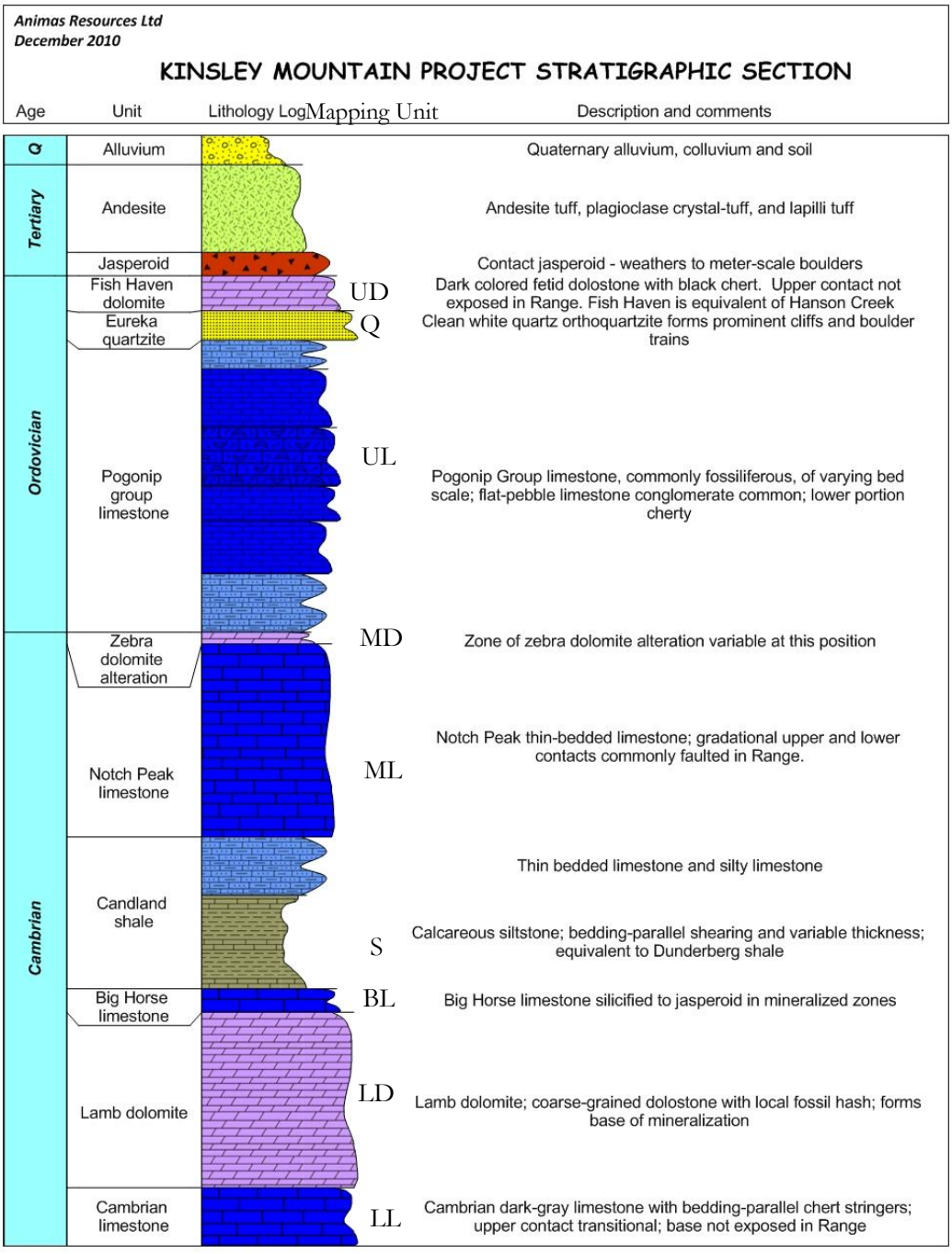

Figure 12. Simplified stratigraphic column for Kinsley Mountain. Abbreviations for mapped units are shown to the right. LL - lower limestone, LD – lower dolostone, BL – bedded limestone, S - shale, ML - middle limestone, MD - middle dolostone, UL – upper limestone, Q – quartzite, UD – upper dolostone (MacFarlane, 2010).

Mapped Unit	Formations/Member
upper dolostone	Fish Haven Dolomite
quartzite	Eureka Quartzite
upper limestone	Pogonip Group
middle dolostone	Notch Peak Limestone
middle limestone	Notch Peak Limestone
shale	Orr Formation (Candland Shale)
bedded limestone	Orr Formation (Big Horse Limestone)
lower dolostone	Lamb Dolostone
lower limestone	Trippe limestone / Abercrombie Formation

Table 5. Table with mapped units from this study correlated with formation or member names.

Lower limestone - Trippe Limestone or Abercrombie Formation.

With only 50 meters of true thickness exposed, the lower limestone unit is the most difficult to confidently correlate with any other regional geological formation. Robinson (2005) thought that this unit could correlate to the Abercrombie Formation. This section occurs in the nearby Deep Creek Range to the east. Further into Utah, below the Lamb Dolomite, the first limestone unit encountered is the Trippe Limestone. Below this unit is then the Abercrombie Formation. The Abercrombie Formation is upwards of one kilometer thick with lithologic variability ranging from shale interbeds to bedded and massive limestone. In White Pine County, Nevada, this unit could correlate with the Lincoln Peak Formation of the Schell Creek and Snake Range

Lower dolostone – Lamb Dolomite.

All previous workers have referred to the lower dolostone as the Lamb Dolomite. In reading descriptions of the Lamb Dolomite of Utah, I agree with the naming of this unit

as Lamb Dolomite. In Nevada, a dolomite occurring at the same stratigraphic horizon is named the Hamburg Dolomite (Coats, 1987).

Bedded limestone and shale – Orr Formation.

During mapping, I used the youngest shale interbed to denote the contact between the shale and middle limestone units. In review of stratigraphic columns for western Utah, the lithologic descriptions for the Orr Formation match my observations (Hintze, 1998). The Orr Formation consists of a basal limestone unit, the Big Horse Limestone (Nutt, 1994). Above this is the Candland Shale, which grades upwards into the Johns Wash Limestone and Corset Springs Shale. This division of the Orr Formation is from the Fish Springs Range in Utah; in the closer Pilot and Deep Creek Ranges, the Orr Formation is mapped but undifferentiated. My observed section at Kinsley Mountain appears to correlate well with the measured section in the Fish Springs Range.

Previous workers at Kinsley Mountain have variably referred to the Cambrian units by different nomenclature. Coats, (1987) mentions that "the Big Horse Limestone member of the Orr Formation is not present further west than Kinsley Mountain" in his report. The Candland Shale has been referred to as the Dunderberg Shale, while the Johns Wash Limestone and Corset Springs Shale have been referred to as the Windfall Formation. According to Robinson (2005), USGS geologists identified trilobite fragments in the basal portion of the middle limestone as *Logannellus* and *Richardsonella.* This would correlate the lower part of the middle limestone to the sub-units of the Windfall Formation. Buckley (1967) recognized and correlated the lower part of this unit with similar units of the Windfall Formation of central Nevada. Robinson (2005), Alta Gold, and Teck Cominco distinguished between the lower and upper portions of the middle limestone, assigning the lower part to the Windfall Formation and the upper part to the Notch Peak Formation. With the use of the term Lamb Dolomite for the unit below and Notch Peak Formation for the unit above, both of which correspond to stratigraphic sections using the Orr Formation

nomenclature, it would make the most sense to refer to these units as members of the Orr Formation.

Middle limestone, middle dolostone – Notch Peak Formation

The Notch Peak Formation at Kinsley Mountain consists of the middle limestone and middle dolostone mapped units. The middle dolostone is further interpreted to be an alteration product that parallels the Cambrian to Ordovician contact at the top of the Notch Peak Formation. The Notch Peak is consistently limey at Kinsley Mountain, while in nearby ranges, the Notch Peak can be wholly dolomitic. All previous workers have referred to the middle limestone as the Notch Peak Formation.

Upper limestone – Pogonip Group.

The upper limestone unit is thought to be in conformable to fault contact with the Notch Peak Formation below. The Pogonip can be distinguished from the underlying Notch Peak Formation as it displays greater stratigraphic variability, ranging from flat pebble conglomerate to siltstone to dolostone.

Quartzite and upper dolostone– Eureka Quartzite and Fish Haven Dolomite.

As the quartzite and upper dolostone make up only a small fraction of the exposed rock at Kinsley Mountain, not much effort was put forth into regional correlation. With that said, Charles Thorman in a field visit to the study area assured me that these units correlate to the Eureka Quartzite and Fish Haven Dolomite, respectively (Thorman, 2010 pers. comm.).

Igneous Rocks

Zamudio (1992) and Gans (1991) document an Eocene (42-40Ma), intermediate composition, extrusive volcanic event in the Dolly Varden (Zamudio, 1992) and Deep Creek (Gans et. al, 1991; $^{40}Ar/^{39}Ar$ from biotite) mountains, ranges immediately east and west of Kinsley Mountain respectively. Nutt et. al. (1994), mentions an $^{40}Ar/^{39}Ar$ age of 40.6 ± 0.1 Ma on volcanics similar in description to those at the southern end of Kinsley Mountain. Buckley (1967) describes the andesitic volcanics at Kinsley as "similar to Oligocene (?) rocks

further south in the Antelope Range".

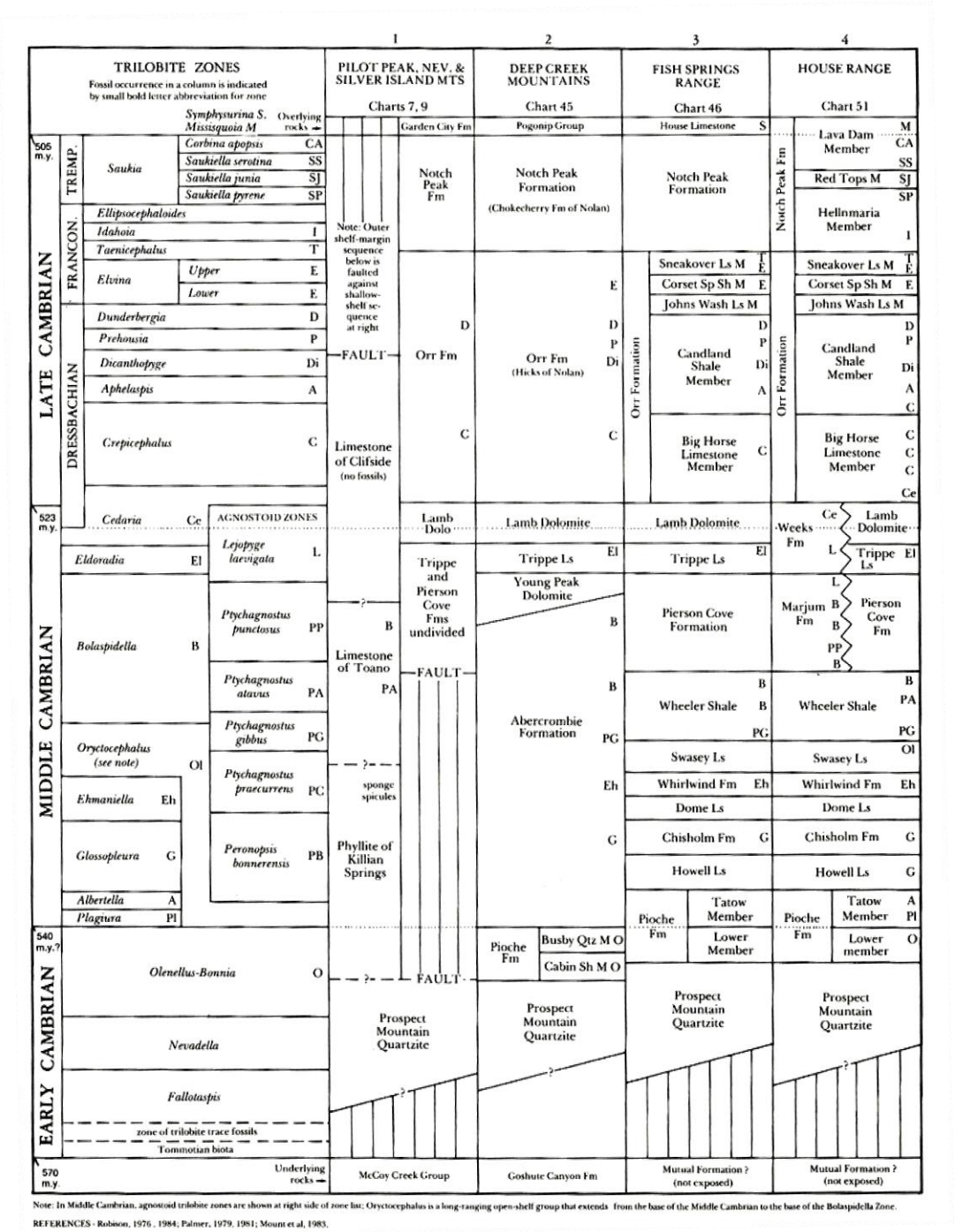

Figure 13**.** Stratigraphic correlation of the Middle to Late Cambrian of western Utah and eastern Nevada as collected from several mountain ranges in a roughly west-east transect (after Hintze, 1988).

The volcanic rocks exposed to the south and west of Kinsley Mountain are designated Tr1 and Ta1 on the Geologic Map of Nevada, compiled by the USGS (Crafford, 2007), both of which are considered lower Oligocene to middle Eocene (23-48 Ma). Maldonado et. al. (1988) determined the exposed quartz monzonite and monzonite porphyry to the south to be 33.4-35 Ma. Since the andesites lie atop thermally altered rocks associated with the exposed quartz monzonite stock, the andesite must be younger than 34Ma. If however, the radiometrically determined age of the stock is incorrect, which may be the case as several phases and dike sets similar in composition to the andesite cut the stock, then the andesite could be older than 34Ma. In the southern Goshute-Toano range, John Wilson and I (2010) visited Jurassic quartz monzonite bodies that have a strikingly similar appearance to the Kinsley Mountain stock. If the Kinsley Mountain stock were Jurassic, the resetting of the age could be related to later uplift of the rocks during Tertiary extension or local sources of andesite, which must have increased the heat flow in the immediately surrounding areas.

Conclusion

One of the challenges facing exploration companies at Kinsley Mountain is uncertainties pertaining to which unit should be expected when drilling below the Lamb Dolomite. With only 50 meters of thickness exposed, little information can be gathered from the surface. The most important conclusions to come from this study of the Kinsley Mountain stratigraphy is a model of which rock units could be encountered in drilling below the Lamb dolomite. Upon completion of this study, I would agree with Robinson (2005) that the Abercrombie unit is likely at the base of the Kinsley Mountain section. This means that although this unit has no mineralization in the exposed 50 m of true thickness at the surface, with the Abercrombie Formations thickness in excess of 1 kilometer, other favorable horizons for ore deposition likely exist. This is omitting structural complications, which will be discussed in chapter III.

Chapter 3

STRUCTURE

Regional Structure

Kinsley Mountain and the surrounding mountain ranges have undergone a complex structural evolution. Kinsley Mountain is situated between the Antler and Sevier orogenies in the Mesozoic fold and thrust belt (figure 14). Previous workers have delineated multiple contractional deformations, including attenuation structures (Thorman, 2010; Silberling and Nichols, 2002; Ketner et. al.,1998; Nutt and Thorman, 1994; Welsh, 1994, Hintze, 1988), regional-scale folding (Silberling and Nichols, 2002, Miller and Gans, 1989), and both top-to-the-east and top-to-the-west tectonic transport (Silberling and Nichols, 2002). To further complicate the history, strike-slip faulting (Thorman, 2010; Nutt and Thorman, 1994) and at least two stages of extensional deformation, are also documented throughout northeast Nevada. Previous work on low angle extension in the region includes work by (Howard, 2003; Silberling and Nichols, 2002; Muntean et. al., 2001; Gans et. al., 1991; Miller and Gans, 1989), while high-angle normal faulting has been investigated by (Rahl et. al., 2002; USGS Online, Ketner et. al., 1998).

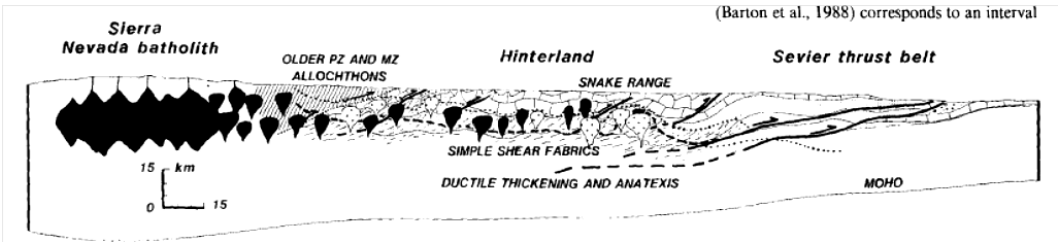

Figure 14. Cross section from the Sierra Nevada to the Wasatch Front with tectonic provinces illustrated. (After Miller and Gans, 1989).

The structural progression of northeast Nevada and northwest Utah have been divided into several regional deformation events. Beginning in central Nevada, the earliest contractile events to affect the region were the Antler, Humbolt, and Sonoma orogenies. Nearly continuous progressive deformation then began to migrate eastwards, with the

Central Nevada Fold and Thrust belt exemplified by the Elko orogeny. The continued eastward migration evolved into the Sevier orogeny (Figure 15). Figure 15 from DeCelles (2004), shows the timing and spatial associations of this contractional deformation in an east-west transect across northern Nevada and Utah. Following the cessation of contractional deformation, a period of relaxation and collapse of the Mesozoic highlands occurred in two stages of regional extension. The first of these extensional events was accommodated by metamorphic core complexes, typified by low-angle, large separation normal faults. The last regional deformation event to affect the region, which is still an ongoing process, is the Basin and Range event with characteristic high-angle normal faulting.

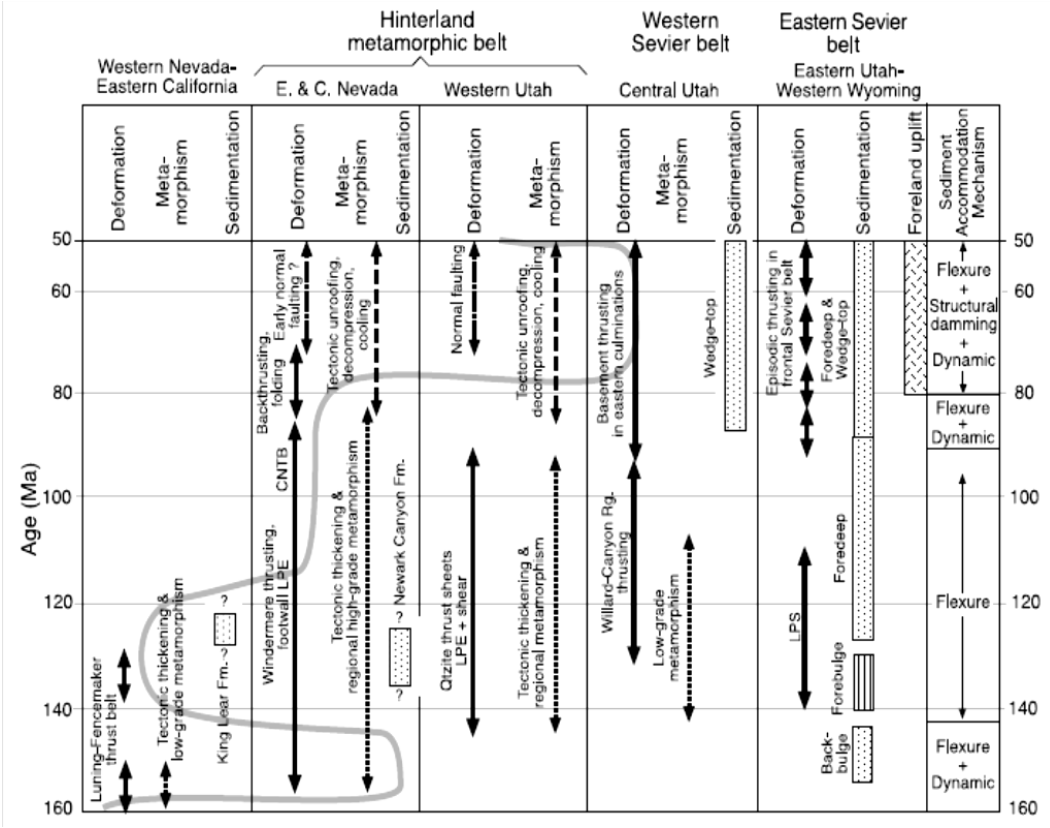

Figure 15. West to east structural progression across Nevada and Utah. (After DeCelles, 2004).

Antler, Humbolt, and Sonoma Orogenies

The Antler, Humbolt, and Sonoma Orogenies were the first post-miogeoclinal deformational events to effect northeastern Nevada. The locus of this deformation was accommodated in central to western Nevada and is best expressed by the Luning Fencemaker thrust belt (LFTB). The most famous structure associated with this event is the Roberts Mountain Thrust. This structure has been extensively studied as world-class gold deposits of the Carlin trend are mostly situated in structural windows beneath this thrust plane. Although these compressional deformations occurred at different times in geologic history, they have been grouped here as the effects of these deforming events is not well expressed in eastern Nevada and western Utah.

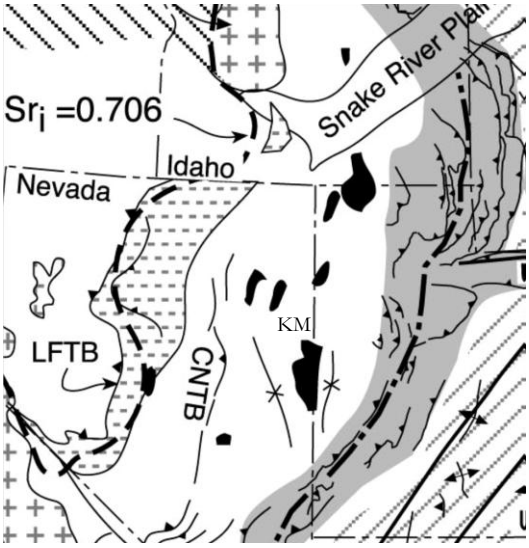

Figure 16. Tectonic provinces of Nevada and Utah with the location of Kinsley Mountain (KM) approximated. Modified from DeCelles, 2004.

Central Nevada Fold and Thrust Belt

The Central Nevada Fold and Thrust Belt records the onset of the eastward migration of compressional deformation from central Nevada to present day west-central Utah. DeCelles (2004) describes this region as "a series of north south-trending thrusts and folds… bracketed between Permian to Mid-Cretaceous". USGS field geologists have

carefully defined a separate orogenic event that affected this region. This event, known as the Elko orogeny (Thorman et. al., 1992; Thorman and Peterson, 2004, Thorman, 2010) deforms rocks east of the Roberts Mountain Thrust and west of the Wasatch Front. The Elko orogeny can best be described as an east-directed contractional deformation with both older-over-younger and younger-over-older faulting. Tear faults oriented west to west-northwest are associated with differential movement during the above mentioned contractional event. The total contraction of the crust has been determined to be on the order of 15-20%, much less than that of the Antler and Sevier orogenies, to the west and east respectively (Thorman, 2010). The Elko orogeny is constrained by cross-cutting relationships involving regional fabrics, igneous rocks, and stratigraphic units (Silberling and Nichols, 2002).

Sevier Orogeny

The Sevier orogeny is a belt of mostly thin-skinned thrust faults and associated folds that terminate at the Wasatch Front. DeCelles (2004) mentions that the east-west distance covered by the Sevier event is ~300 km, with a north-south distance in excess of 2000 kilometers. West of (behind) the Sevier belt is the "hinterland", a zone of complex deformation and metamorphism. Figure 16 shows the spatial relation between the Sevier front and the Hinterland, within which Kinsley Mountain is situated. It is likely that deformation associated with this tectonic event occurred at Kinsley Mountain.

Metamorphic Core Complex Development

The mid-Tertiary low-angle extensional event is represented in northeastern Nevada and western Utah by the formation of metamorphic core complexes. Two of these complexes, the Snake Range – Deep Creek and Ruby Mountain – East Humbolt complexes, expose basement rocks of Precambrian age and exhibit penetrative fabrics. Extension occurred perpendicular to the older contractional events with extensional overprinting of older fabrics (Howard, 2003). The magnitude of separation along these structures is on the

order of tens of kilometers. The result of the core complex is that high-grade metamorphic basement rocks are juxtaposed against younger, less deformed rocks. In the nearby Deep Creek Range, a decollement structure places high-grade metamorphic units against younger less deformed rocks.

Basin and Range Event

The Basin and Range tectonic province stretches from the Snake River Plain in the north to Mexico in the south. It is characterized by a series of north-south-trending or northwest-trending high-angle normal faults. The alternating nature of the horst and graben structures results in elongate basins and ranges. Some of the basins can reach depths in excess of 3,000 meters. This extensional event is still an active, ongoing process in northeastern Nevada and western Utah. Some of the basin fill material is offset by normal faults dipping towards the basin. Some of these basins do not develop perfect horst and graben structures, but develop half grabens when only one side of the range has accommodated the extension.

The general style of each regional deformation event have been recorded and documented in the ranges surrounding Kinsley Mountain. The regional structural history, summarized from the literature includes, from oldest to youngest: $D1_{regional}$ intrusion-related bedding parallel shearing, $D2_{regional}$ bedding-parallel attenuation structures, $D3_{regional}$ regional-scale folding, $D4_{regional}$ low-angle extension, and $D5_{regional}$ high-angle extension. $D1_{regional}$ has been documented in the Goshute-Toano Range (Silberling and Nichols, 2002; Ketner et. al., 1998). $D2_{regional}$ bedding parallel attenuation structures have been documented throughout northeast Nevada and northwest Utah. Workers have identified this style of deformation in the Goshute-Toano, Deep Creek, and other nearby ranges (Thorman, 2010; Silberling and Nichols, 2002; Ketner et. al., 1998; Thorman, 2010 pers. comm.). $D3_{regional}$ folding has been documented in the Deep Creek, Kern, Goshute-Toano, and Cherry Creek mountain ranges (Silberling and Nichols, 2002; Ketner et. al., 1998). This event resulted in mountain-scale

anticlines and synclines, which are generally upright and open, but can be inclined with limbs that approach vertical. The $D4_{regional}$ event is well documented in the nearby Snake Range to Deep Creek Range fault system (Miller et. al., 1999) and Ruby Mountains metamorphic core complex (Howard, 2003; Wannamaker and Doerner, 2002; Satarugsa, 2000; Miller and Gans, 1989). The final event, $D5_{regioal}$ is characterized by high-angle normal faults that can be found in all mountain ranges in the region. This event is currently active throughout the Great Basin, with movement along the Wells Fault within the past 10 years (Thorman, 2010 pers. comm.). The USGS documents Quaternary faulting in most ranges surrounding Kinsley Mountain (Dohrenwend et. al., 1991).

Structure of Kinsley Mountain

A variety of structures affect the Cambrian through Ordovician sedimentary rocks of Kinsley Mountain. These structures, from oldest to youngest are: 1) bedding parallel shear zones and patchy cleavage, 2) a north-northwest striking cleavage, 3) open folding-trending north–northeast and northwest tear fault, 4) low-angle, west-dipping normal fault, 5) east-west and northwest high-angle normal faults, 6) north-south oriented high-angle normal faulting.

The structural history of Kinsley Mountain is recorded by cross cutting relationships preserved in the rocks. The major events recorded by these rocks are contractile deformation, followed by younger extension. At least two generations of both groups of structures have been identified in the Kinsley Mountain study area, as well as the surrounding ranges. Kinsley Mountain is located just north-northwest of the highly extended terrain of the Snake Range to Deep Creek Range fault complex. Other mapped decollement faults exist north of Kinsley Mountain in the Goshute-Toano range. Another well-studied metamorphic core complex in the Ruby Mountains, about 50 miles northwest, further emphasizes the effect of Mid-Tertiary extension on the region. Figure 17 shows the tectonic history of Kinsley Mountain in a series of block diagrams.

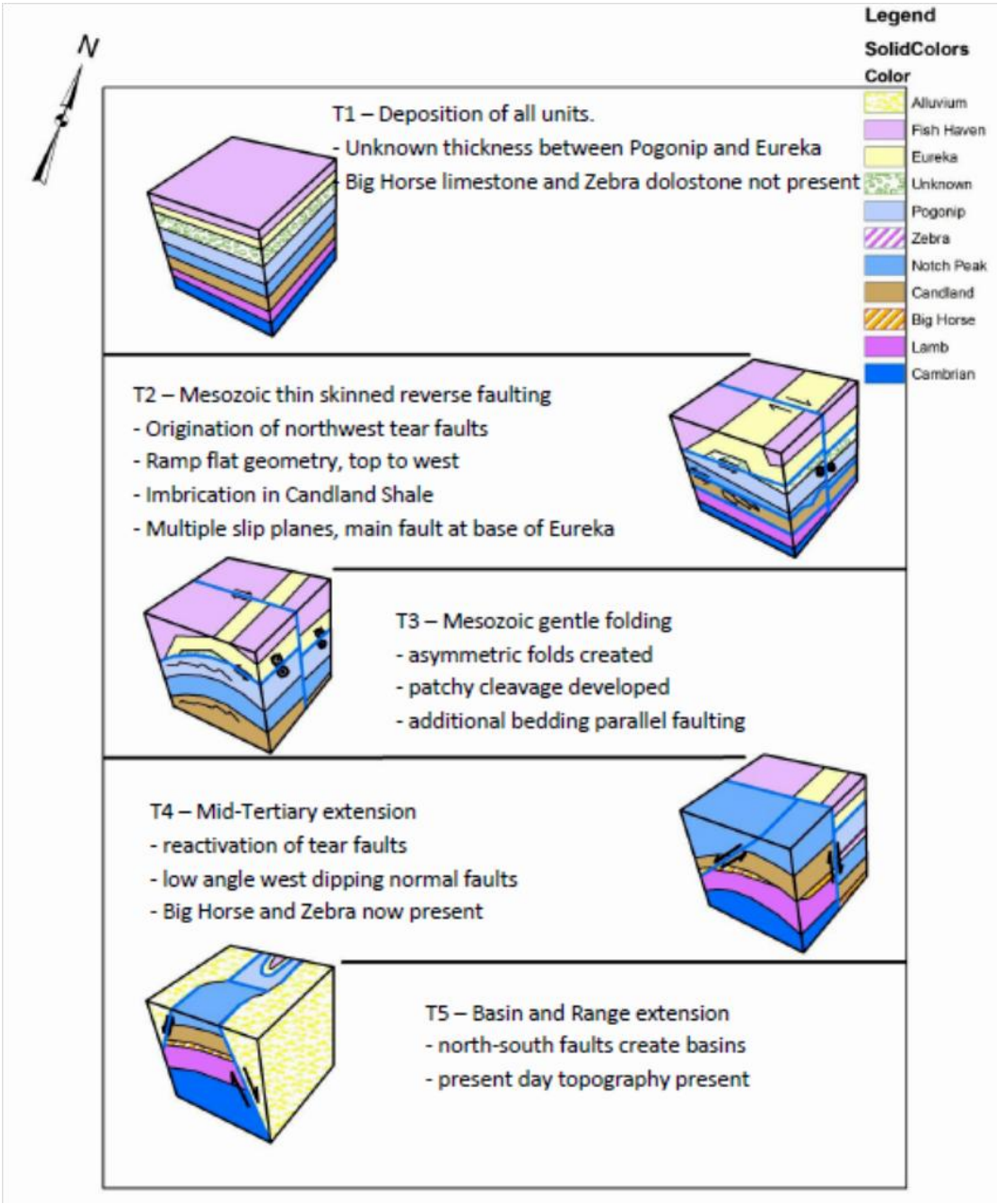

Figure 17. Block diagrams illustrating the tectonic history of Kinsley Mountain. (MacFarlane, 2010).

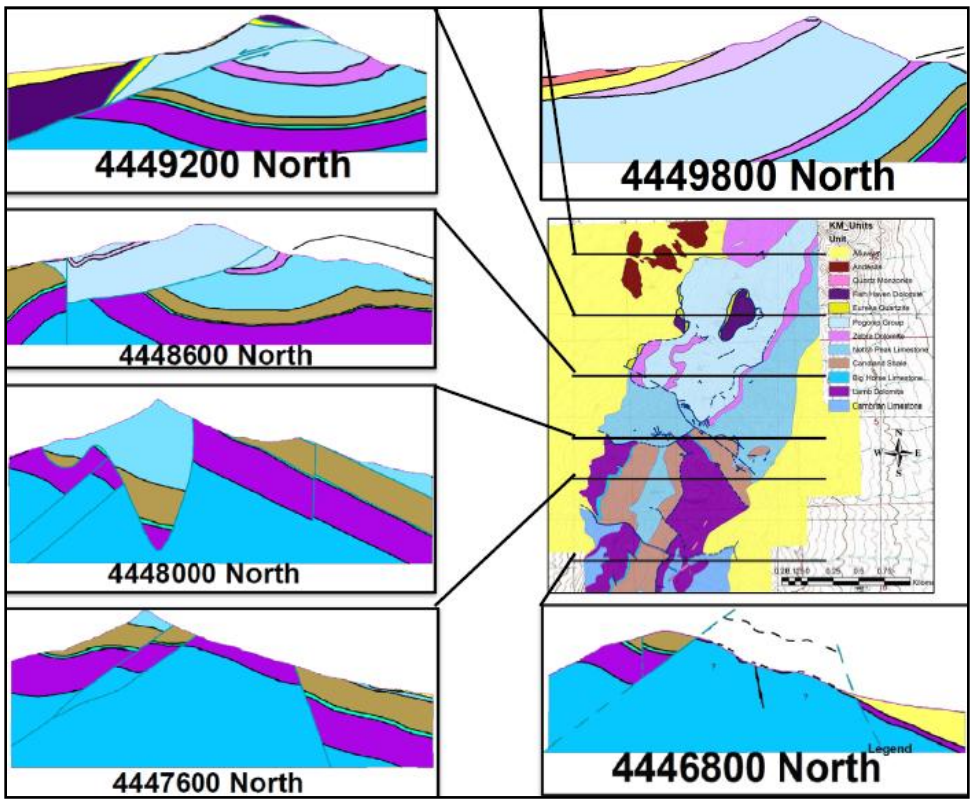

Figure 18. East-west cross sections illustrating structural levels and deformation events from south to north along the range. No vertical exaggeration (MacFarlane, 2010).

D1 - Bedding Parallel Structures

The oldest structures observed are bedding-parallel shear and cleavage zones, which can also display brecciation and gouge formation. The fabrics, where best developed, display S-C textures, as well as boudinage of originally continuous beds (figure 19). These structures occur throughout the sedimentary sequence with contacts between units accommodating the majority of the deformation. Two contacts, the Lamb Dolomite to Big Horse Limestone and the Pogonip Group to Eureka Quartzite, display the most intense deformation from this event. The thickness of individual beds within the carbonate units also displays some control to the intensity of this event, with thinly bedded limestones displaying stronger bedding parallel cleavage than more massively bedded limestones or dolostone (figure 19). These cleavages were later enhanced by decalcification. Away from the man-made exposure

of the pits, bedding-parallel structures are more difficult to recognize unless stratigraphy has been removed (figure 3), as weathering rates are enhanced by the additional permeability.

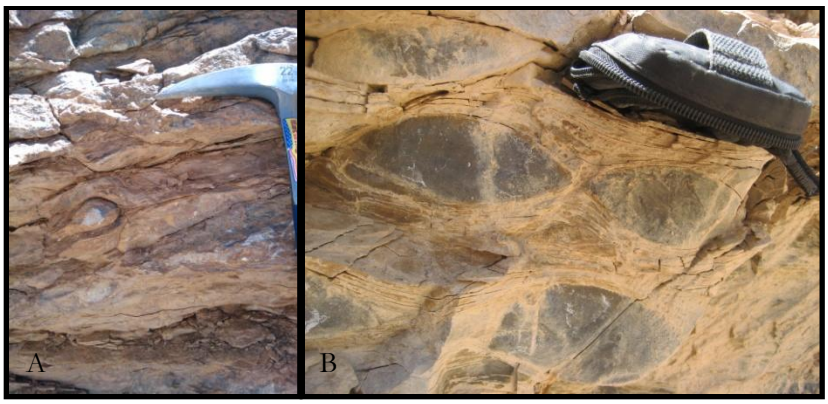

Figure 19. Well developed bedding parallel shear later enhanced by decalcification. Images from the Lower Main pit.

Bedding-parallel structures strike north-northeast and dip gently southeast in the southern part of the range and gently northwest in the northern part of the range. Anastomosing shears can be observed in the Main Pit, where they produce meter-scale boudins. The shear zones have attenuated the stratigraphy to an unknown degree and can completely remove units, as best expressed by the Big Horse Limestone within the Main Pit. In the Candland Shale, limestone lenses from several centimeters to half a meter display boudinage (figure 19) resulting in limestone sigmoids "floating" in sheared and cleaved shale.

The bedding-parallel faulting is interpreted to be compressive, even though it resulted in younger-over-older displacements. The event responsible for the attenuation of the stratigraphy included: variably intense cleavage development, unknown amounts of possible east directed movement and an overall increase in the permeability of the sedimentary sequence. The magnitude of attenuation ranges from removal of the ~**5**m thick Big Horse Limestone, up to a maximum of greater than 1 km potentially attenuated between the Pogonip Group and Eureka Quartzite. Other factors that may have contributed to the thinning of the sedimentary package cannot be ruled out and include paleotopography and Paleozoic arches.

D2 - Fold and Thrust

D2 deformation within the Kinsley Mountain project was a brittle-ductile event that resulted in local imbrication of more massive limestone beds and asymmetric folding of thinner bedded limestone and shale. A weakly developed, spaced cleavage is exposed in the Main Pit. This S2 cleavage is roughly axial planar to the asymmetric, small-scale, F2 folds. Figure 20 is an image of transport indicators related to the D2 event. In figure 20A, asymmetric folds can be seen to verge in a top-to-the-west direction (photo looking north). This occurs near the faulted contact between the upper shale unit of the Orr Formation and the Notch Peak Limestone. In figure 20B, more massively bedded limestone near the same contact, responded to the deformation with small-offset, imbricated thrust faults. The break in figure 20B from black (above) to brown (below) is the deformed contact between the Candland Shale and Notch Peak Limestone.

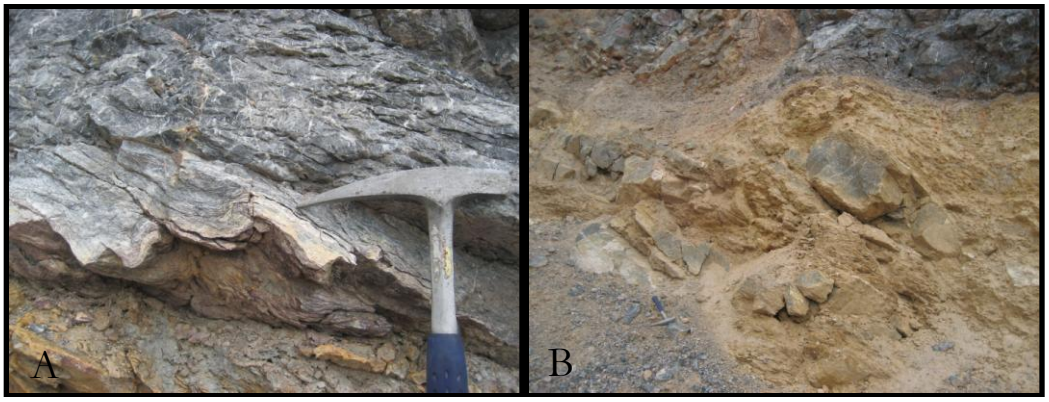

Figure 20. D2 transport indicators within the Main Pit indicating top-to-the-west displacement.

A spaced cleavage developed in response to the D2 deformation. This cleavage strikes ~N20-35E, roughly parallel to the overall fold axes, and dips gently to moderately east. This cleavage cuts across bedding at a low-angle, as shown in figure 21. In figure 21, bedding is shown by the dark gray (limestone) paralleling the head of the hammer, while the

S2 cleavage is oriented from top right to bottom left of the image cutting bedding at ~25°. This image was taken in the Main Pit towards the middle of the Candland Shale section.

Figure 21. Image from the Main Pit of S2 cleavage cutting across bedding (S1 is not present at this location). Bedding is shown with black lines, while cleavage is shown with blue lines.

D3 - West vergent, large-scale folding

D3 deformation at Kinsley Mountain resulted in the development of range-scale, gently northeast-plunging folds. This large-scale folding is responsible for the overall dip of the stratigraphy. The result of this deformation is that beds generally dip towards the southeast in the southern part of the study area, but dip northwest in the northern part of the study area. No cleavage has been recognized with this generation of folding. Figure 22 shows the contoured poles to planes of bedding measurements. The shape of the lobes shows that the folding is slightly asymmetric (Marshak and Mitra, 1988). Fitting these poles with a girdle and determining the beta axis shows that the folds gently plunge (03°) towards a 051 azimuth. This stereographic determination of the fold hinge agrees with direct measurements made in the field of smaller scale folds.

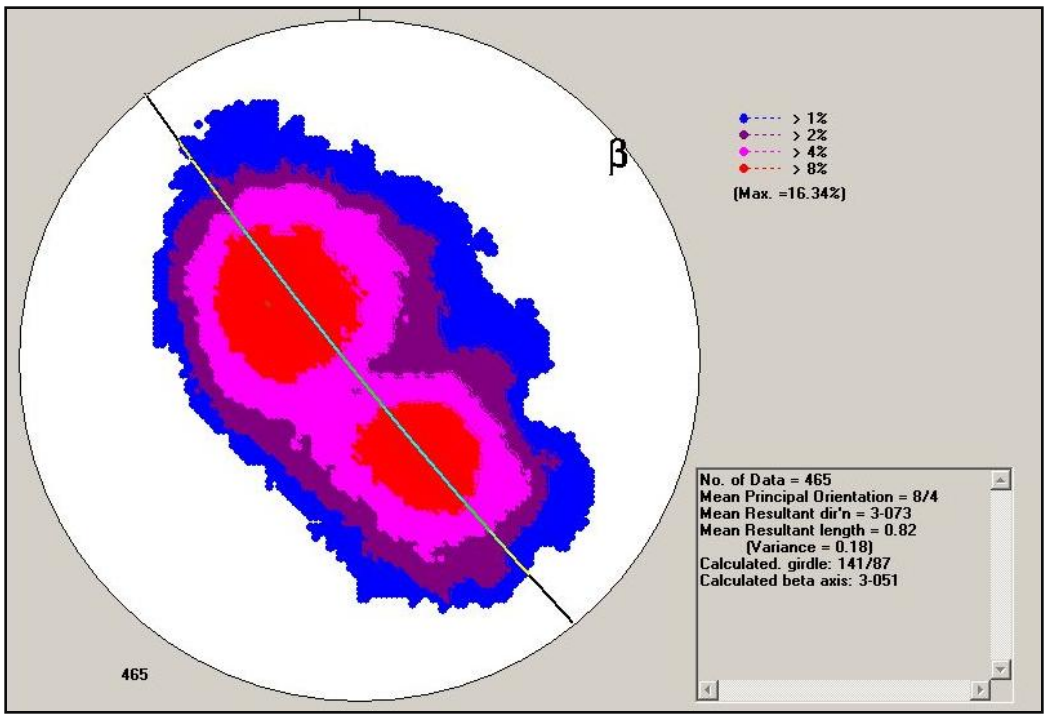

Figure 22. Stereonet (Allmendinger, 2006)with poles to planes of bedding plotted and fit with a girdle, the pole of which approximates the trend and plunge of the large scale fold axes.

D4 – Early Normal Faults

One set of low-angle normal faults cuts through Kinsley Mountain (Snake Fault). These structures can be traced to the south along strike for 1.5 kilometers, where they merge into one structure. This family of structures was determined to be normal faults based on observed displacement of units and drag folding of the beds into a fault-parallel orientation. The stratigraphic seperation along these structures varies between 350-550 meters, with more total seperation occurring where the single fault bi-furcates into parallel structures. The Snake Fault (figure 3) strikes 030 and dips 35˚ NW on average. These low-angle structures cut across a bedding-parallel cleavage just south of the study area (figure 23). In this photograph the view is facing southeast, perpendicular to the strike of the fault. This structure is interpreted to be a normal fault although clear offset was not determined in the field.

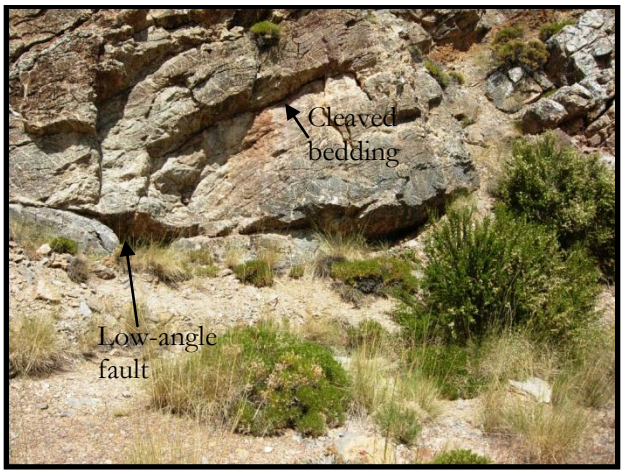

Figure 23. Low-angle structure interpreted to be a normal fault cutting across bedding-parallel cleavage. Photo taken just south of the study area on the west slope.

D5 – Later Normal Faults

A set of northwest-striking, high-angle faults are the next structures to affect Kinsley Mountain. These structures are brittle faults with normal movement and left-lateral separation. The separation is due to the low inclination of the beds, while the significant younging across these structures is indicative of normal offset. These structures strike between 270 and 310 with steep dips consistently to the northeast or near vertical. Two of these structures were mapped across the range: the Strip Fault and the Cross Fault (figure 3). Previous geologic maps show another parallel structure just south of the study area (Buckley, 1967). These structures are associated with minor silicification and jasperoid development, as well as paralleling vein swarms of both quartz (in dolostone) and calcite (in limestone) that increase in intensity as D5 structures are approached. This deformation event, accompanied or followed by erosion, is responsible for the continued younging of stratigraphy to the north throughout the mapped portion of the Kinsley Range.

This generation of structure is present along the mined strip, where all of the deposits are located within close proximity to these faults. The actual fault planes or stratigraphic breaks associated with D5 do not contain mineralization, but instead appear to truncate and dismember mineralization. Jasperoids and breccias associated with this event

generally do not host mineralization. Mineralized fragments can be observed in breccias associated with these structures.

D6 – Late-Stage Normal Faults

On the east side of the range, the Boundary Fault (figure 3), an east-dipping normal fault, is a brittle structure with hematite-stained soils. It was determined to dip east by its interactions with topography and by an alignment of topographic saddles with visibly increased iron-oxide content. This structure approximates the bedrock to colluvium contact and is thus interpreted to be a basin-bounding fault. In their study of Quaternary faulting in Nevada, the USGS concluded that the east side of the Kinsley Range, specifically north and south of the study area, is an east-dipping basin-bounding fault with Quaternary movement (Dohrenwend et. al., 1991). This latest stage of extension is thought to be responsible for the shaping of the present day topography and is still an active, ongoing process.

Discussion of Structure

Bedding-parallel faults have been mapped in the Cherry Creek and Goshute-Toano Ranges, to the east and north respectively. Some controversy surrounds the timing of these structures, as previous investigators have called them Mesozoic (Hintze, 1988; Thorman and Peterson, 1994; Silberling and Nichols, 2002), while others have pinned Tertiary ages (Silberling et. al., 1997) to the structures. The Tertiary age was assigned due to the removal of stratigraphy or attenuation of the "normal" stratigraphic section; in Silberling's original model, the removal of stratigraphy had to be extensional. Within the Kinsley Range, these-bedding parallel structures are related to a patchy cleavage development, which in turn is folded by later compressional deformation, necessitating that these structures occurred early in the structural history of the range. On a small scale, individual beds can be attenuated or boudinaged, and it is possible that this same process may occur on a larger scale, although more work would be necessary to say with confidence this has occurred.

D2 deformation consists of east-dipping thrust faults with minor offset and the patchy development of fault-parallel cleavage. This event is likely similar to the $D3_{regional}$ event of Silberling and Nichols (2002), which displays east-dipping, localized structures associated with west-northwest vergent folds. At Kinsley Mountain, these west-northwest vergent folds are regarded as the D3 event.

The D3 event at Kinsley Mountain may correlate to the D2 event recorded in the White Horse Pass terrain of the Goshute-Toano Range to the north (Silberling and Nichols, 2002). In the Goshute-Toano Range, the large-scale fold takes the form of a regional syncline. At Kinsley Mountain, the next range to the south of the Goshute-Toanos, the regional structure takes the form of a broad anticline. In the Spruce Mountains northwest of Kinsley, a syncline is present that is potentially related to the same event. Also, in the Cherry Creek Range to the south of Kinsley Mountain, Silberling and Nichols (2002) mention unpublished data of northeast-trending folds in Mississippian rocks. Other west-vergent fold structures have been documented in the Pequop Mountains and Currie Hills, both northwest of Kinsley Mountain (Wilson and Dennis, 2006). The trend of the anticline at Kinsley Mountain plunges 3 degrees at a 051 azimuth as determined by fitting a girdle to the poles of the planes of bedding measurements (figure 22). Field determination approximated the structures more northerly, gently plunging towards ~030-040.

The timing of D4 structures was determined based on cross-cutting relations, where low-angle normal faults 1) cut across the large scale fold and older cleavage(s); 2) are cut by high angle northwest faults; 3) are preferentially silicified, presumably during mineralization. Since the low-angle normal fault cuts and offsets a 33Ma quartz monzonite dike, these structures are interpreted to regionally correlate with mid-Tertiary extensional event recorded throughout the southwestern United States. Northeastern Nevada was severely affected by this event with some ranges undergoing greater than 100% extension. Two classic examples of metamorphic core complexes exist in the region: 1) the Snake Range, and

2) the Ruby Mountains. The Snake Range is located ~75 kilometers (~50 miles) to the south-southeast, while the Ruby Mountains are located ~100 kilometers (~60 miles) to the west-northwest. Faults labeled as "detachment faults" by the USGS have been mapped in the Goshute-Toano and Deep Creek ranges which are immediately to the north and northeast of Kinsley Mountain. The Snake Fault at Kinsley Mountain is not a detachment fault, but is likely related to the same extensional event that caused core complex formation in the surrounding ranges. Based on others work, it is likely that Kinsley Mountain is in the hangingwall of the more severely extended terrain, as deep ductile fabrics related to this event are not present with the range, but are present to the south, east, and north.

D5 normal faulting occurred in several orientations at different times. The Ridge Fault is thought to represent an early phase of this event, as it is cross cut by the N60W Strip Fault (figure 3). Both structures accomplish north-side down displacement, with stratigraphy younging from basal Windfall to Pogonip Group limestones across the structure. Although the Strip Fault is the best exposed example of this generation of structures, the Cross Fault and others to the south are related to the same event. This set of structures is the most important from the perspective of gold mineralization, as it was the main host to the cave-fill replacement mineralization of the Ridge, Upper Main, and Main (?) pits.

Cave-fill sedimentary units associated with the Cross Fault are horizontally bedded, while similar cave-fill material in the Main Pit are dipping at approximately 40 degrees to the east. This suggests that the cave-fill sedimentary units in the Strip Fault, like the surrounding stratigraphy, have been folded by the D3 (?) event. Furthermore, this indicates reactivation along the Strip Fault with the first movement creating the sedimentary cave fill, while the second movement re-brecciated the older mineralized cave-fill sedimentary units. Not only is this critical for understanding the structural history of the Strip Fault, but it also brackets gold mineralization between the two faulting events that occurred along this structure. The

second generation of northwest-trending faulting, manifested as reactivation of the Strip Fault and the origination of the Cross Fault (figure 3), occurred post-folding of the cave fill sediments. If cave fill is associated with this structure, one would expect any sediments that accumulated in caves to be horizontal as no rotation or folding has occurred after the formation of the Cross Fault. This is what is observed, where bedded cave fill associated with pre Cross Fault caves (along the Strip Fault) is folded and post Cross Fault infill is horizontal. From these timing indicators, the Strip Fault is interpreted to have originated during the D1 bedding parallel, thrust faulting event as an accommodation fault. It was later reactivated during the Tertiary as a normal fault with north-side-down movement. Jasperoid associated with this movement postdates the silicification event, as the matrix includes silicified fragments, although some remobilization (?) of silica occurred along the Cross Fault where it intersects other structures.

Structural Conclusion

The relative timing of deformation events have been worked out for Kinsley Mountain. This sequence of events involves an early phase of contractional deformations with associated faulting, folding, and cleavage development. This was followed by a later phase of extensional deformations involving normal faults of variable orientation, inclination, and magnitude of offset.

This study also determined that multiple movements occurred along the northwest strip, which originated as an accommodation structure during Mesozoic contraction, but had the latest movement reactivating the plane as a normal fault in the Tertiary. This has huge timing implications, as these movements potentially bracket the gold mineralization event. The different cave fill materials give clues about the relative timing of movement along this structure.

Chapter 4

ALTERATION AND MINERALIZATION

Regional Alteration and Mineralization

Gold mineralization in northeastern Nevada and western Utah has been determined by radiometric methods to have occurred in the Mesozoic and Tertiary. The difference in the ages and styles of emplacement has resulted in alteration signatures characteristic of each episode. In general the older systems are richer in base metal and silver than are the younger systems. The age of mineralization in the mountain ranges surrounding Kinsley Mountain spans from Jurassic to Eocene.

Mesozoic mineralization in Nevada and Utah is responsible for numerous large metal occurrences. These include porphyry copper and associated peripheral precious-metal deposits. Alteration of the host rock associated with Jurassic intrusions includes the development of skarn, potassic alteration, and hydrothermal breccias with associated quartz. Several of the younger Carlin type mineral deposits have spatially associated Jurassic intrusions (Cortez Hills and Bald Mountain trend).

Jurassic mineralization in Nevada and Utah is typically associated with igneous activity and results in poly-metallic, base-metal-rich deposits. The Bald Mountain and Gold Hill deposits, of Nevada and Utah respectively, are Jurassic in age (Robinson, 1993; Lee, 2004). The Dolly Varden stock and associated copper mineralization is either 165 Ma or 134 Ma. Both ages have been determined, Jurassic (165Ma) by Zamudio and Atkinson (1992) and Cretaceous (134Ma) as reported on the Viking Minerals website. The Cretaceous age is a date of the Melrose Stock, which is spatially associated with mineralization. Cretaceous mineralization is present at the nearby Robinson mine in Ely, Nevada, which primarily produces copper with anomalous gold and molybdenum. This porphyry-type mineralization is associated with a large alteration and mineral halo.

Tertiary mineralization in Nevada and Utah typically consists of disseminated gold deposits, but the Bingham porphyry copper deposit is also Tertiary. The largest gold deposits in Nevada are those of the Carlin trend. This mineralization is temporally and spatially associated with Eocene igneous activity (Muntean, 2011), but is also spatially associated with the 158 Ma Goldstrike stock. The maximum age to mineralization in the Carlin district is given by Jurassic-Cretaceous mafic dikes that are sulfidized by mineralizing fluids (Teal and Jackson, 2002). The world-class Bingham porphyry copper deposit in western Utah is a Tertiary event with age determinations of Cu and Mo mineralization at 38 Ma (Sillitoe, 1990). Along with copper, the Bingham deposit also has distal disseminated gold in economic concentrations at the Barney Canyon deposit.

Tertiary mineralization in Nevada and Utah is most well known for the formation of Eocene Carlin-type deposits. Carlin-type, distal disseminated, sediment-hosted, gold mineralization occurs in several belts in northeastern Nevada that generally trend north to northwest. Figure 24 shows the trends of Carlin-type mineralization throughout north-central and north-eastern Nevada. To date, an excess of 100 million ounces of gold has been extracted, with an additional 100 million ounces of known gold mineralization remaining in the ground in northeast Nevada. Typical elemental associations with Carlin-type gold mineralization include arsenic, mercury, antimony, thallium, and tellurium. Lead, zinc, molybdenum, and tungsten are typically not associated with gold in Carlin-type systems. Along with this elemental suite, gold concentrations in Carlin-type deposits are typically equal or elevated in comparison with silver concentrations (Teal and Jackson, 2002). The deposits are structurally controlled in most cases and occur in bedded calcareous units, with gold as micron-size inclusions in sulfide minerals. Alterations characteristic of Carlin-type deposits include decalcification (removal of calcium carbonate), argillic alteration, and silicification with the development of jasperoids (Teal and Jackson, 2002; Christensen, 2010 pers. comm.).

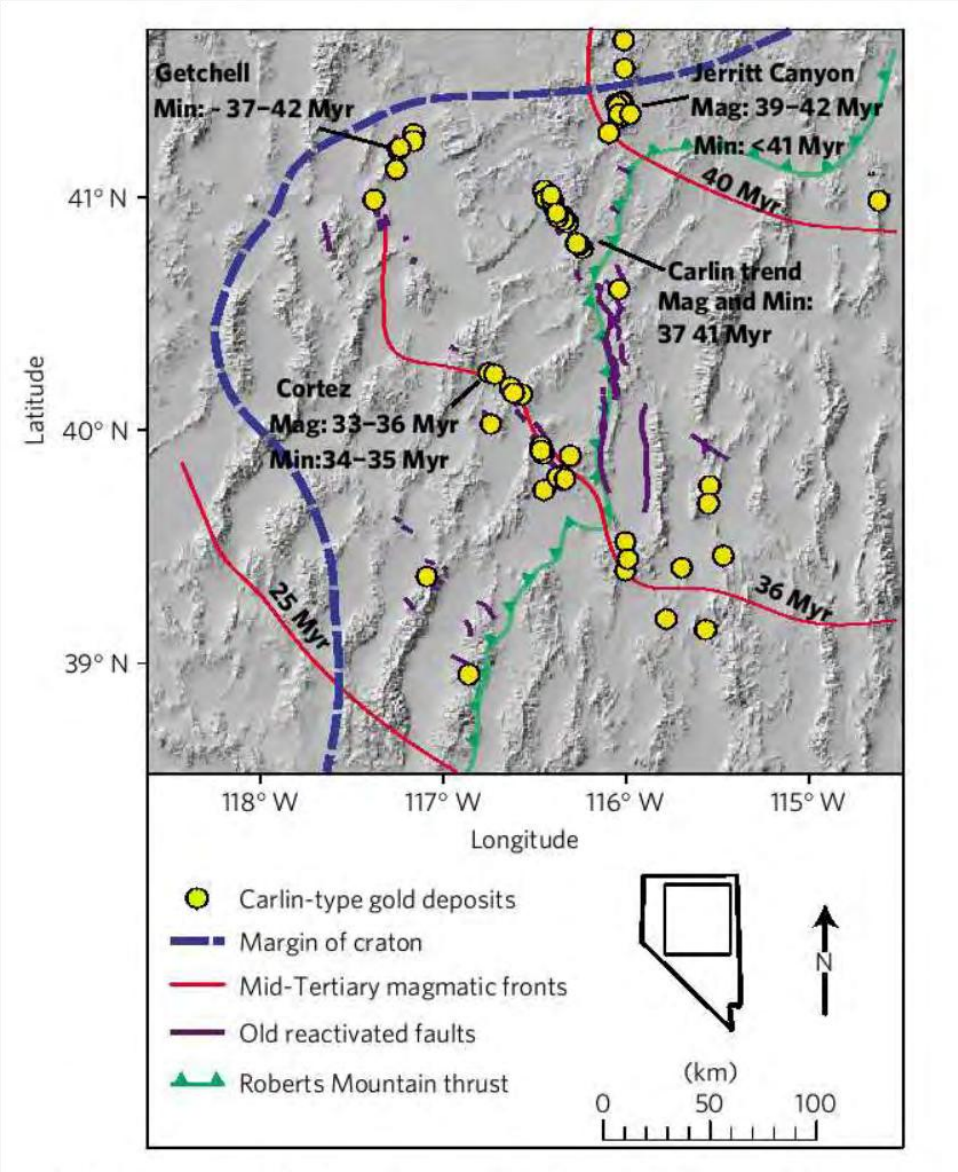

Figure 24. Map highlighting trends of Carlin-type gold deposits in northern Nevada. (Muntean et. al., 2011).

Kinsley Mountain General

Three styles of gold mineralization are present within the Kinsley Mountains, listed in decreasing abundance: replacement of dirty carbonates, silicification or jasperoid associated, and contact metasomatic type. These styles of gold mineralization were identified by geochemical variations, alteration products, grade of mineralization, and the units that were affected. The most important style from the perspective of gold deposition

is the replacement type. Decalcification is the most important alteration associated with gold mineralization, closely followed by silicification. This study focused on identifying and mapping different types of alteration and mineralization present.

Alteration

Alteration at Kinsley Mountain is dominated by two types; decalcification and silicification. The most intense decalcification is near the mined strip. Silicification occurs throughout the mapped area in various forms, which were delineated in this study. The strongest decalcification resulted in the development of caves and other karst features. These sites are also commonly silicified to various degrees and were host to the mined deposits. Other large-scale alteration types present include the zebra banding of the Cambrian/Ordovician contact and the non-destructive replacement of the Big Horse limestone for large strike distances. There are local zones that were altered to clays (argillic alteration) and others overprinted by chlorite and epidote. Although decalcification and silicification are the most important alteration types with respect to Au mineralization, the less common alteration types may give clues about the mineralizing fluids. While mapping, the various alteration types were identified and documented on a relative intensity scale from 0-3, while veins were mapped by estimated percentage of total rock volume. The following are detailed descriptions of each alteration type illustrated with photos and intensity maps.

Decalcification

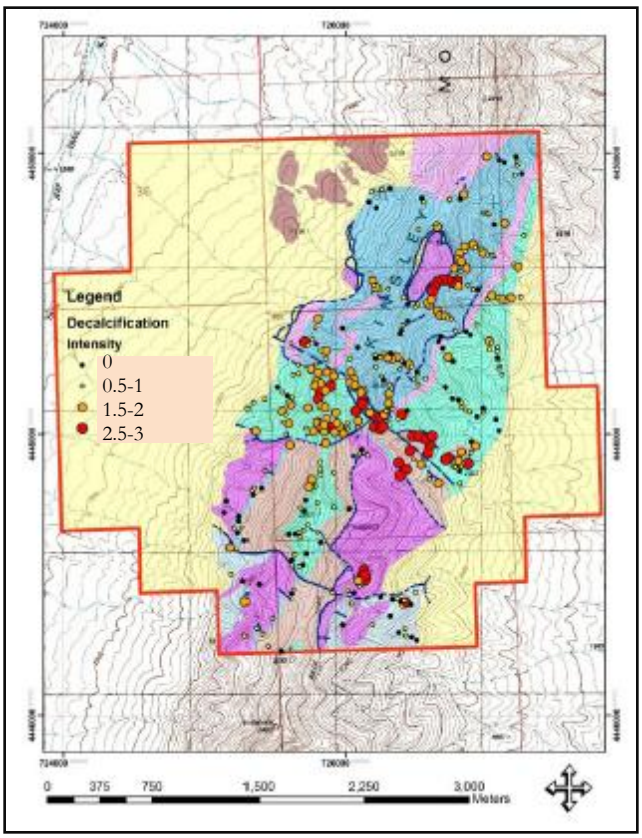

Figure 25. Decalcification intensity map with red dots representing the most intense alteration and black the weakest.

Decalcification was mapped on an intensity scale from 0-3 (figure 25). Examples of the different intensities can be seen in figure 25, where 0 corresponds to unaltered limestone, while 3 corresponds to cave formation and/or severe disruption of primary stratigraphy by removal of material. Odie Christensen and I developed the decalcification scale from several days of field discussion at the onset of the mapping part of this study.

In figure 26, the white boxes illustrate the intensity of decalcification. This image also demonstrates the drastic differences in alteration intensity that outcrops within close proximity can display (image A). The approximate breaks of the intensity scale go from unaltered rock (intensity=0), progressing to bedding parallel decalcification with insoluble

Figure 26. Range of decalcification intensities observed during this study.

residuum (intensity=1). As the intensity of the alteration increases, the thickness of the bedding-parallel residuum widens and begins to coalesce across bedding planes (intensity=2). As the intensity increases further, small pockets begin to form (lower right of image B) and eventually these pockets coalesce into caves (intensity=3).

Where highly decalcified rocks are observed in outcrop, they are limited in size to several meters. Strongly altered rocks have a low preservation potential due to preferential erosion and burial resulting in poor exposure. Original bedding thickness and permeability (faults and karst) at the time of mineralization are thought to be the most important contributors to the intensity of decalcification. Figure 25 illustrates the structural control to

decalcification with the mined strip displaying the strongest intensity. To the north, a series of low-angle structures interpreted as thrusts are moderately to strongly decalcified. To the south of the mined strip decalcification is confined to structures and commonly associated with silicification. Sites that are preferentially decalcified are a combination of northwest small offset structures and the intersection with changes in. The contact between the Lamb Dolomite and Cambrian limestone can be intensely decalcified.

Although the decalcification driven by hydrothermal processes can be very destructive to the original calcareous lithologies, caves may, in part, be a result of surficial karst-forming processes. Caves and the resulting cave fill sediments, which were the primary sites of limestone hosted gold mineralization, indicate several successive generations of cave formation (figure 27).

Surficial karsting may have occurred during the Cambrian-Ordovician periods, although this event has not been clearly identified in the field. Two generations of cave formation have been identified and are separated by the main gold event. Figure 27 shows the two defined generations of cave formation. The older event is shown in Figure 27-A

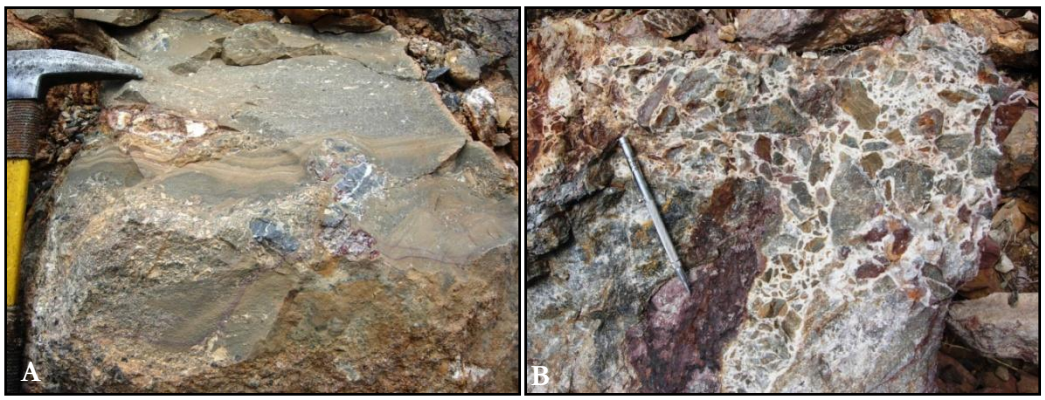

Figure 27. Two generations of cave fill are present throughout the study area, an older (A) and a younger (B) generation. Both of these images are from the road between the Main Pit and Upper Main Pit.

which shows episodic infill of the cave with alternating fine material and course debris. This implies that this generation of cave fill may have developed by karsting. This generation of

cave fill is preferentially silicified and hosts gold mineralization. Figure 27-B shows the younger variety of cave fill material. This material is angular and generally matrix supported, locally consisting of mineralized and altered fragments. The matrix of this generation of cave fill consists of coarsely crystalline calcite. This matrix calcite is also cut by fine quartz veinlets. The young generation of cave fill is generally not mineralized with the exception of fragments of older mineralization. The younger generation may be formed through hydrothermal processes associated with reactivation of faults along the mined strip.

Silicification

Several distinctive types of silicification have been observed and mapped within the study area. These have been separated to include quartz flooding, silicified fault breccias, replacement of bedding or cave-fill material, and contact silicification. These types of silicification are distinguishable in the field. The following are detailed descriptions of each type of silicification in decreasing order of importance to gold mineralization.

Of the different types of silicification identified, the replacement style had the closest association to gold mineralization. Of the two types of replacement silicification, bedding-replacement and cave-fill replacement respectively, lithology controls which type is present. Silicified cave-fill material is most common in the areas surrounding the mine and only has been observed in limestone lithologies. Bedding -replacement silicification preferentially affects the Big Horse Limestone unit. This unit can be variably replaced for strike lengths greater than 1 km with associated low-grade gold mineralization. Fault zones, like the west-dipping Snake Fault (figure 3), an extensional fault that places Candland Shale next to Lamb Dolomite south of the mine area, also display bedding-replacement silicification. The silicification is controlled by the fault but completely replaces the adjacent

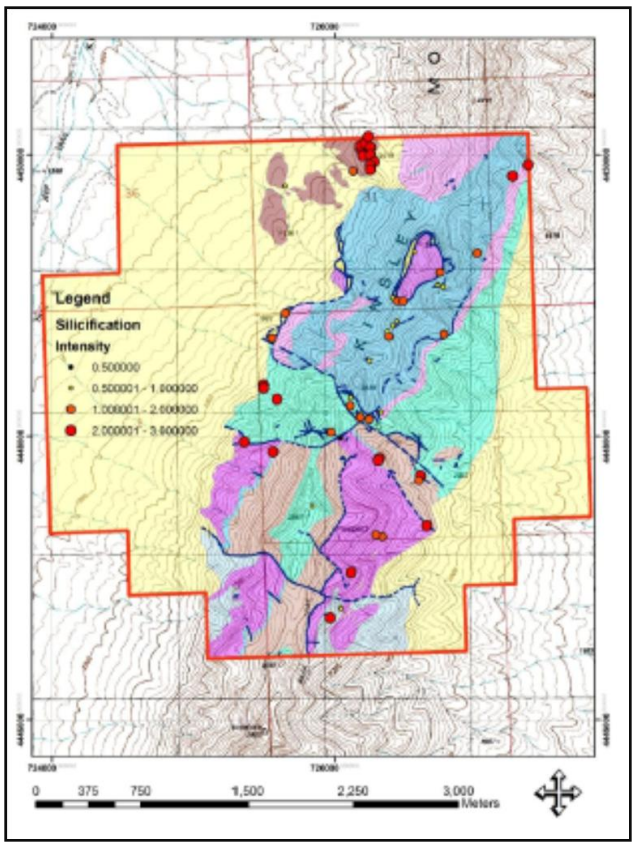

Figure 28. Map with the distribution and intensity of silicification as defined during outcrop mapping. MacFarlane (2010).

Replacement Silicification

units over 2-3 m, even preserving primary sedimentary structures in the shale. This type of silicification can carry low-grade gold and is likely related to the hydrothermal system.

Silicified Fault Breccia

Silicified fault breccias occur within several orientations of faults, but occur frequently along northwest-trending structures ranging from 270-360 azimuth. The thickness of these breccias is highly variable, ranging from 3 cm to 10 m wide along the same structure. Although it is clear in the field that the main control on the silicified breccia is the orientation of the fault, these breccias locally share characteristics of the other varieties of silicification. These include local pods of stockwork quartz (observed when structure cuts dolostone), bedding-replacement silicification (where structures cut Big Horse Limestone), and cave-fill replacement. Figure 29-A shows one of the larger silicified fault breccias

encountered. This one occurs at the intersection of a NW fault and the Big Horse Limestone. At the base of this jasperoid, arsenic and iron oxides are present (figure 29-B) but gold values are low.

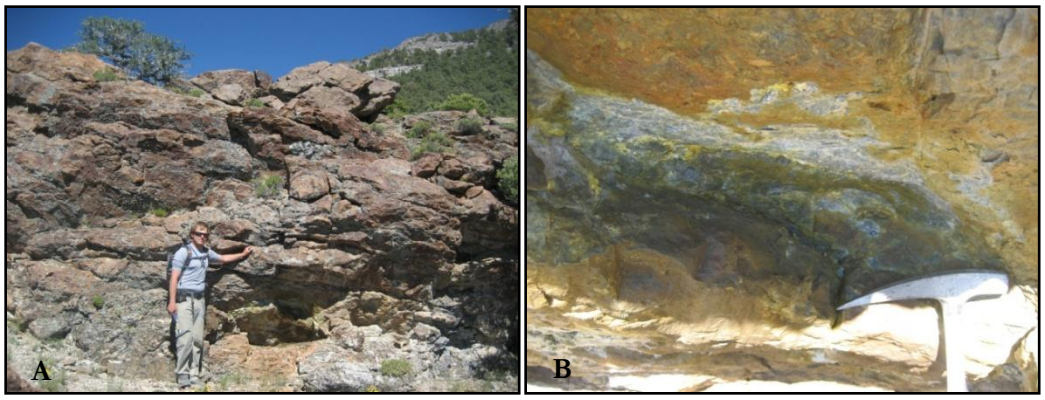

Figure 29. Fault breccia and replacement intersection jasperoid. These images are from the west slope, south of the Mined Strip.

Quartz-Vein Flooding

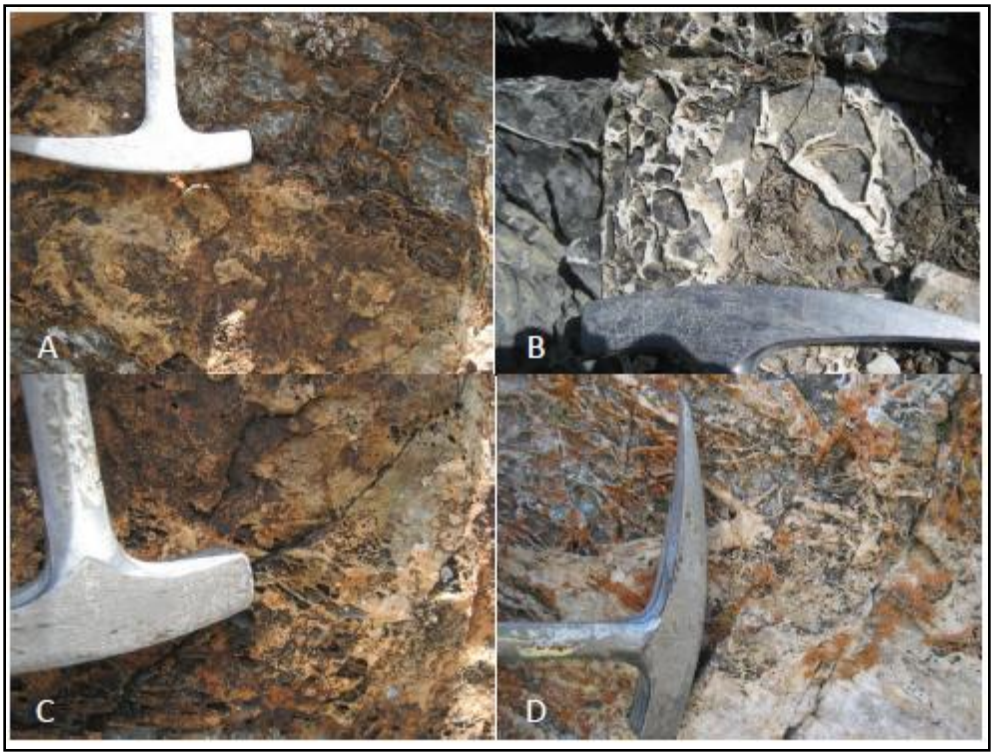

Figure 30. Various observed intensities of quartz-vein flooding from the Lamb Dolomite south of the Mined Strip. Image A shows quartz stockwork in upper right grading into quartz flooding. Image B shows quartz veins as matrix to a crackle breccia. Image C shows fragments of stockwork quartz in a zone flooded with quartz. Image D shows the sharp gradation from quartz stockwork to quartz flooding.

Quartz-vein flooding is best developed in the Lamb Dolomite, but also occurs in silicified fault zones. Quartz veins are the only vein type present within dolomitic units. These quartz veins can increase in intensity as both structures and the quartz monzonite dikes are approached. Figure 30 shows the range of quartz-vein intensities observed within the Lamb Dolomite. This quartz-vein flooding has been observed in all stages of development. It ranges from individual hairline quartz veins to a crackle breccia (B). This can then become a quartz stockwork and increase further into 1m wide quartz veins with remnant stockwork inclusions (C). In figure 30A a zonation from individual veins increasing in intensity from upper right to bottom left into quartz flooding. These veins were sampled in an area of intense stockwork at the furthest north exposure of the quartz monzonite dike with resulting gold content below detection limits.

Contact Silicification

Contact silicification occurs in the northern part of the study area. Silicified boulders occur stratigraphically at the base of the andesite. Where the andesite blanketed the landscape and was overlying limestone, brecciated jasperoids developed. Where the andesite was in contact with dolomite, no jasperoid developed. Remnant limestone cores have been observed in thin section examination of these fragments by Odin Christensen (2010, pers. comm.). Geochemical sampling has shown this type of silicification to have no potential for gold mineralization.

Veins

Detailed mapping of vein types and vein intensity was conducted over the study area as shown in figure 31. This mapping was conducted in an attempt to define patterns that could vector towards exploration targets. No clear vector was defined, but some general spatial relations have been observed. Two factors most affect the type and intensity of veins; these are lithology and proximity to either a structure or an intrusive rock. Quartz and

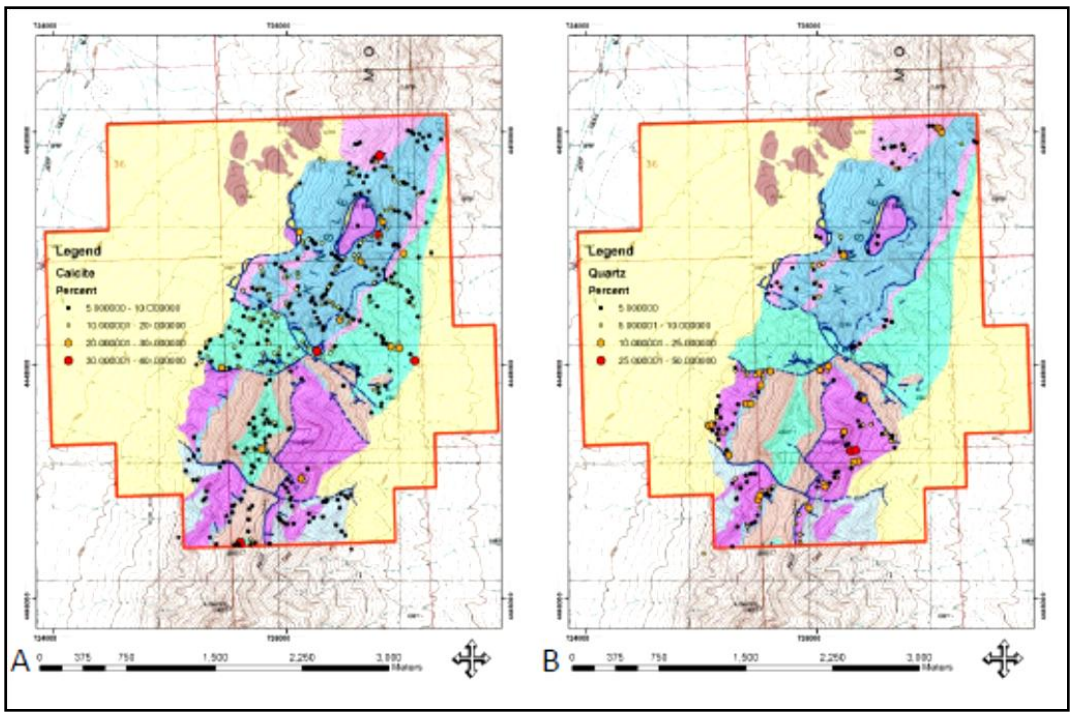

Figure 31. Maps with the intensity of calcite (A) and quartz (B) veins recorded in estimated volume percentages as defined during outcrop mapping.

dolomite veins are generally restricted to dolomitic lithologies, whereas calcite veins are present throughout the range (figure 31). The types of veins present in decreasing abundance are: calcite, quartz, dolomite, and pink calcite possibly rhodochrosite. The intensity of veins, both calcite and quartz, can vary from non-existent to upwards of 40% of the total volume of rock. Veins range in thickness from 1 mm-10 cm with variable strike length.

Argillic

Argillic alteration of the calcareous lithologies is not common within the Kinsley range, but the andesitic volcanics weather intensely into clay. Where argillic alteration is encountered in calcareous lithologies, it is not very large in size and is primarily restricted to fault zones in siliciclastic rocks or in dirty limestones of the Pogonip Group. Clay alteration has been observed in the Main Pit at the sheared contact between the Lamb Dolomite and Candland Shale (Big Horse Limestone is missing).

Epidote and Chlorite

Epidote and chlorite are minor alteration products in the study area. Epidote and chlorite have been observed in two forms: along fractures and pervasively disseminated. Both types are also associated with silicification with the fracture-type occurring on the margins of quartz-flooded jasperoid. The pervasive type is less common, but is associated with pervasive silicification of the outcrop where observed. In an outcrop west-northwest of the Ridge Pit, along the northwest trend of the mined pits, the pervasive epidote and chlorite is best developed as shown in figure 32. It replaces finely bedded limestones and is pervasive in this outcrop but only along fractures in nearby outcrops. One sample was taken and contained 0.8 ppm gold mineralization, potentially relating the gold, epidote, chlorite, and silicification to a low temperature alteration process associated with intrusive activity. The epidote and chlorite are likely the low-temperature signature of a distal intrusion.

Discussion of Alteration

Of the two dominant alteration types in the Kinsley Range, decalcification of the calcareous lithologies is more restricted to areas of mineralization than is silicification.

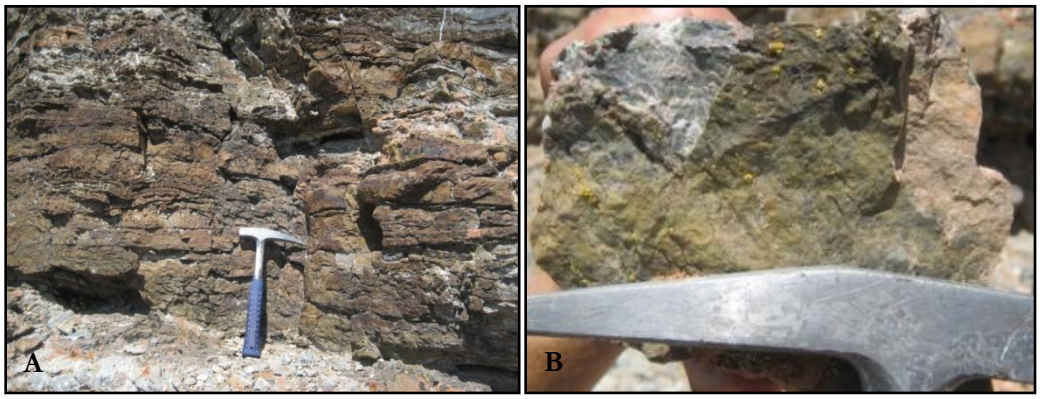

Figure 32. Pervasive (A) and fracture coating (B) epidote and chlorite alteration. These photographs are from outcrops along the Strip Fault on the western slope.

Decalcification occurs to varying intensities based on the lithology and distance from large structures. The process of decalcification is interpreted as a product of both surficial karsting

and a low temperature hydrothermal event. The decalcification results in a zonation towards the fluid pathway, which is usually a structure. The fluid pathway typically has a silicified core with shells of variably intense decalcification and calcite veining decreasing in intensity away from the central silica core (figure 33-A).

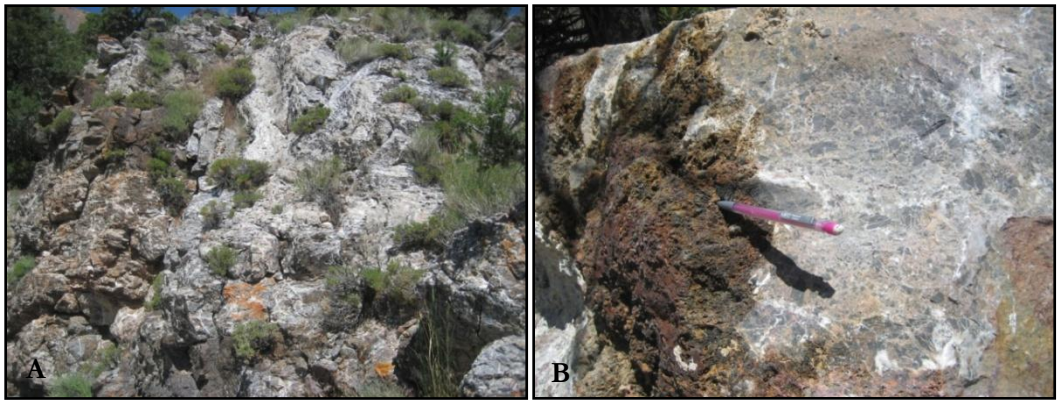

Figure 33. Cave zonation occurring at various scales. Image A-shows zonation on 10's of meter scale, whereas B-shows zonation on meter scale. These images are from the dump (B) and valley just north of the dumps on the east face of the mountain, north of the Mined Strip.

Figure 33-A is an outcrop scale silica pod north of the lower pits that most clearly displays the zonation from a silica-rich core outward to intense calcite veining and eventually grading into average calcite vein density over 10-40 m. This zonation goes from a silica and silicified breccia core with removal of carbonate outward into remobilized calcite veining. This then grades outward into a few calcite veins per meter to nearly no veins present. Figure 33-B shows zonation of alteration grading from the central silica core through stockwork veining into relatively unaltered rock over 1m. The scale of this zonation may vary in accordance with the size of the central silica zone but is on the order of meters to 10's of meters or more.

The silicification event that affected the older stage of cave fill is associated with gold mineralization. Since the caves do not appear to be deformed by the compressional deformation they are younger than the deformation. The earliest stage of cave formation and cave fill is bracketed between compressional deformation and mineralization. This

means that the responsible process could be surficial karsting, or early stage hydrothermal decalcification. The highest density of known caves occurs along the mined strip, which is controlled by a series of northwest-trending structures. The multiple generations of cave formation could be evidence of multiple movements along the controlling northwest set of structures. Since calcite veins have been observed to be zoned around the edges of caves, it is likely that the hydrothermal event (low temperature mineralizing fluids?) was responsible for driving the cave forming process through decalcification of limestone.

Cross-cutting relations and field associations allowed for a general sequence of alteration events to be determined. It was noted that calcite veins both cut and are cut by bedding-parallel decalcification. This is interpreted to indicate several stages of calcite veining. Since the style of the calcite veining and its lateral association to decalcification is a repeated pattern, it seems plausible that they are a continuation of the same event. Since these cave fill breccias and sediments were later silicified and mineralized, this puts a cave formation and infilling event between the main stage decalcification and mineralization events. Epidote and chlorite, where observed, are associated with silicification, thus relating these events. It seems plausible that all the observed alteration is all related to one igneous driven system. Cross cutting relationships exist between calcite veins, caves, and silicification. These are likely a result of the leading edge of a hydrothermal system which decalcification of limestones was controlled by colder fluids that were moving away from the heat engine, while later higher temperature fluids deposited chlorite, epidote, and silicification in caves and limestones.

Mineralization

Gold mineralization at the Kinsley Mountain is present in two distinctive types: bedding replacement and silicification of cave-fill sedimentary rocks. Although there are two forms of gold mineralization, similar alteration associations are present, including decalcification, silicification, and proximity to a major structure. Over the length of the

mined strip, this relation is clearly displayed with the upper deposits taking the form of silicification and replacement of cave-fill materials. In the lower pits, the gold mineralization took the form of bedding-parallel replacement associated with silicification. Both forms of gold mineralization display a gradational zonation of gold grade, from a central high-grade core that progressively decreases over several meters to uneconomic grades. Both types of mineralization style occur along the same structure, with the controlling difference being the lithology present. The bedded limestones tend to form caves with infill sediment while the moderately cleaved Candland Shale and basal Big Horse Limestone tend to be preferentially replaced. The gold partitions into the shale, most likely along fractures and bedding planes, while the silica preferentially replaces the Big Horse Limestone.

Visible copper, molybdenum, and zinc mineralization were encountered at the margins of the exposed quartz monzonite intrusion to the south of the Animas claim. Hand samples returned grades up to 1.66% Cu, 1.35% Pb, and 1.435% Zn, all of which were sampled along fractures that strike 020 and dip vertical to steeply to the east in visible mineralization. Along the margins of the main intrusive body, there is thin poorly developed skarn and hornfels. There is garnet skarn present along the contact of the intrusive, but no visible metals were directly associated with this skarn, but rather were restricted to the above-mentioned fractures. While tracing a northeast dike from the main intrusive body across the study area, garnet magnetite skarn <0.2 m with minimal iron oxides and traces of copper mineralization was observed. The final exposure of the dike crops out within 200 m of the Lower Main pit. Within this pit, several pieces of quartz monzonite were found in the rubble but none was observed in outcrop.

This study utilized the collection of soil, rock-chip, and stream sediment samples to gain insight into the mineralization process. Through analyzing multi-element geochemical data using several approaches, this study aimed to find elemental associations to mineralizing events. The analysis techniques used for the soil dataset were determination of correlation

coefficients and a factor analysis. For the rock chip and stream sediment samples, only correlation coefficients were determined. All of these data were visualized with the aid of a graphical information system (ArcGIS).

Soils

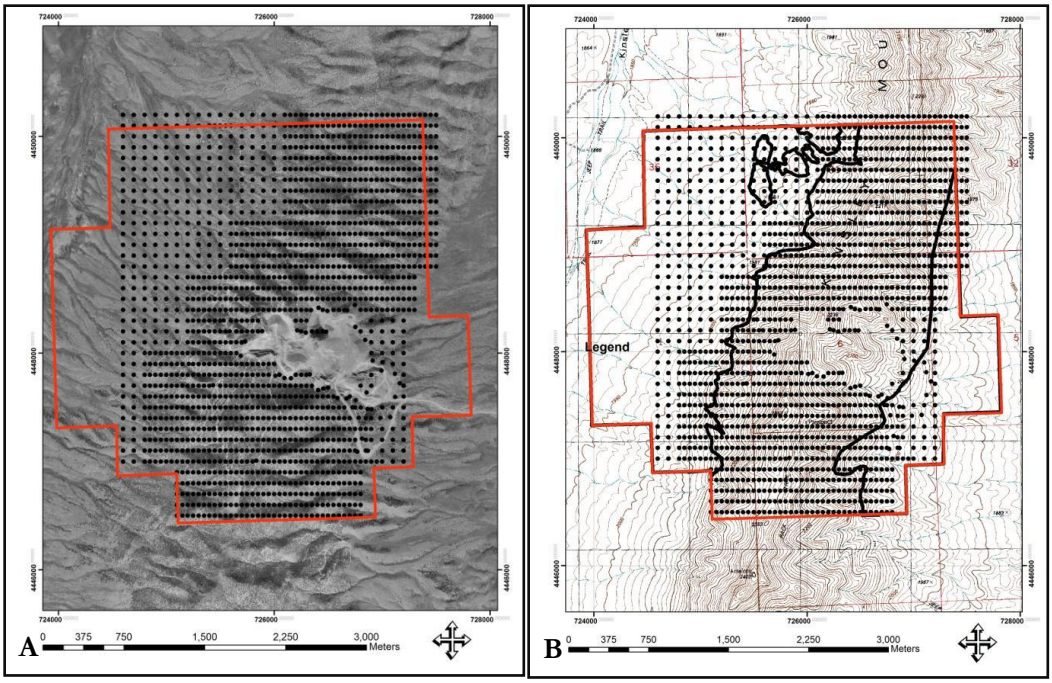

Figure 34. Images of the soil sampling grid over an air photo (A) and topographic (B) base layer with black points representing collection locations.

Soil sampling was conducted over the study area as illustrated in Figure 34. The only holes in the grid were within the highly disturbed pits and over the mine dumps. A total of 1610 samples were collected; these were then analyzed for multi-element geochemistry. The spacing of the grid pattern over the bedrock portions was 50 m by 100 m. In the alluvial cover, the grid spacing was adjusted to 100 m by 100 m (figure 34). The geochemical package was a 51 element suite offered by ALS Chemex. The highest grade gold sample returned was 1 ppm, with greater than 1% of the total assays returning at >0.1 ppm gold.

The multi-element assays from the soil geochemistry survey were examined using statistical analysis software. The soil-survey dataset was chosen as it contained the highest number of samples and showed the greatest variance, both of which are important factors

for meaningful statistical analysis. The method used was a combination of correlation scores and factor analysis.

Statistical Analysis

Soil Correlations >0.5	**Au**	**Ag**	**Cu**	**Mo**	**Zn**
	Te	Cd, Pb (0.67), Zn	Bi, -Ca, Co, Cs, Fe, Mn, Ni, Rb, Y	Tl (0.55)	Ag, Cd, In, Pb
Soil Correlations >0.7	**Au**	**Ag**	**Cu**	**Mo**	**Zn**
	Te				Cd, In (0.71)
Soil Correlations >0.8	**Au**	**Ag**	**Cu**	**Mo**	**Zn**
	Te (0.80)				Cd (0.91)
Weaker correlations					
Au	Ag (0.15), As (0.40), Hg (0.22), Mo (0.17), Sb (0.13), Tl (0.29), W (0.16)				
Ag	Cu (0.26), In (0.44), Mg (0.28), Mn (0.35)				
Mo	Au (0.17), As (0.24), Hg (0.17), W (0.19)				

Table 6. Correlation coefficients of various elements determined from the soil data set.

Correlation Coefficients

From the correlation study relations between precious and base metals were of particular interest. These included; Au, Ag, Cu, Mo, and Zn (table 5). Gold displayed a 0.80 correlation to tellurium and a 0.40 correlation to arsenic. There is a significant drop in the next group of correlations, with those related at >0.10 being Tl, Hg, Mo, W, Ag, and Sb. Although the correlations are very low, some of these are included in the suite of elements that are most commonly associated with Carlin-type deposits (Hg, Sb, and As from above). Silver displayed a strong positive correlation (>0.50) with several of the base metals with Pb, Cd, and Zn being the strongest, although Cu, Mg, Mn, and In also displaying positive correlations >0.25. Lead and zinc are strongly correlated to one another as well as showing a >0.50 correlation with Ag, Cd, and In. Copper, although associated with base metals and silver, is most strongly correlated with bismuth (0.60) and Fe, Mn, Cs, Ni, Co, Rb, and Y. As the correlations approach 0.1, all of the precious and base metals begin to cluster together.

The correlations have relations that are not typical of Carlin-type gold mineralization. The arsenic, mercury, antimony typical of a Carlin-type system displays a poor association to gold. On the other hand, the Te, Tl, Mo, and W suggest an intrusion related source and can be present in, but are not common to, Carlin-type systems. The mineralization source is interpreted to be distal disseminated from a felsic, igneous system, either the exposed quartz monzonite to the south or another non-outcropping intrusion. An important factor that could significantly affect the correlation determinations is the mixing of samples taken in bedrock and alluvium, as these may be shedding insight into primary mineralization and how this mineralization holds together during erosion and transport. For this reason the analysis were determined after separating bedrock from alluvium with no significant changes in the correlation scores. Te remained the most strongly associated element to gold mineralization, with variance of all correlation coefficients <0.03 from the mixed-to-bedrock-only method.

Factor Analysis

Factor analysis was undertaken on the soils dataset as an alternative method for determining relationships and patterns related to mineralization. In order to get the most out of a factor analysis study, a large dataset that displays a moderate to high degree of variation should be used. For this reason the soil dataset was chosen. Within these data however there are varying qualities (low variation) of data present. Elements that have concentrations (well) above the detection limit generally display a sufficient deviation, from which meaningful statistical analysis can be made. The elements that have very low mean concentrations also commonly display very low deviation, thus making statistics including them questionable.

Factor	Elements
1	Al, Be, **Ca**, Ce, Co, Cr, Cs, Cu, Fe, Ga, Ge, Hf, K, La, Li, Mn, Nb, Ni, Rb, Sc, Sn, **Sr**, Th, Tik V, Y, Zr
2	As, Tl, W
3	**Ag, Cd, In, Mg, Pb, Zn**
4	B, S
5	**Au, Te** Bold = positive

Table 7. Table of factor groupings from the soil data set.

The process of factor analysis utilizes eigenvalues to generate factors, leading to a reduction in the dimensionality of the dataset (Piekenbrock, 2009). Through the use of eigenvalues the total number of meaningful factors can be determined. When the curve of Eigenvalues can be fit with an approximately straight line, the limit of meaningful information that can be extracted from the dataset has been reached (Piekenbrock, 2009 pers. comm.). For the Kinsley Mountain soil dataset, the number of meaningful factors that can be extracted was determined to be five. At this point, the eigenvalues of the dataset resemble a straight line. While only 59% of the total data has been accounted for within these first 5 factors, the remaining 41% contains a high percentage of data that has little statistical significance (variance), including some of the rarely encountered elements that were analyzed. In the determination of factors from the data set, the first factor accounted for over 30% of the total data, where the second factor only accounted for 9% of the total data. The remaining factors accounted for successively smaller percentages of the total data.

Table 6 shows the factor groupings from the soil data set. The first factor is interpreted to represent limestone as the only positive factor score is that of calcium and strontium. The remainder of elements in factor 1 displays negative factor scores, indicating that these elements are generally not present where calcium and strontium are. Factor 2, interpreted as the porphyry factor, consists of arsenic, thallium, and tungsten, all of which have negative factor scores. Factor 3, interpreted to be a base metal intrusive signature, consists of positive factor scores for silver, cadmium, indium, magnesium, lead and zinc. Factor 4 consists of boron and sulfur with both having negative factor scores. This factor

could be related to an alteration event that removed both from the host rocks, as may occur distal to intrusive systems. Factor 5, the gold factor, is associated with tellurium, with both elements displaying positive factor scores. This is thought to represent a felsic intrusive source.

From analysis of these data, it appears that at Kinsley Mountain, an intrusive event was responsible for the emplacement of metals. The individual factors, although all interpreted as indicative of intrusive activity, do not reduce any further than five factors. In other words, these five separate factors will not reduce to one factor. Instead they are interpreted to represent proximal and distal signatures of the intrusive event. It cannot be said with any certainty which intrusion was the causative one, either the exposed quartz monzonite to the south or a non-outcropping intrusion.

The base metals lead and zinc score well together, but do not score well with copper. Similarly, the second factor, although interpreted as a porphyry signature, does not include copper. Another surprise is that molybdenum does not group into any of these intrusive related factors. Although elements can be grouped using factor analysis, it does not say anything about the timing or uniquely define the mineralizing source. These interpretations have been put forth as opinions of the author and are not the only solutions possible.

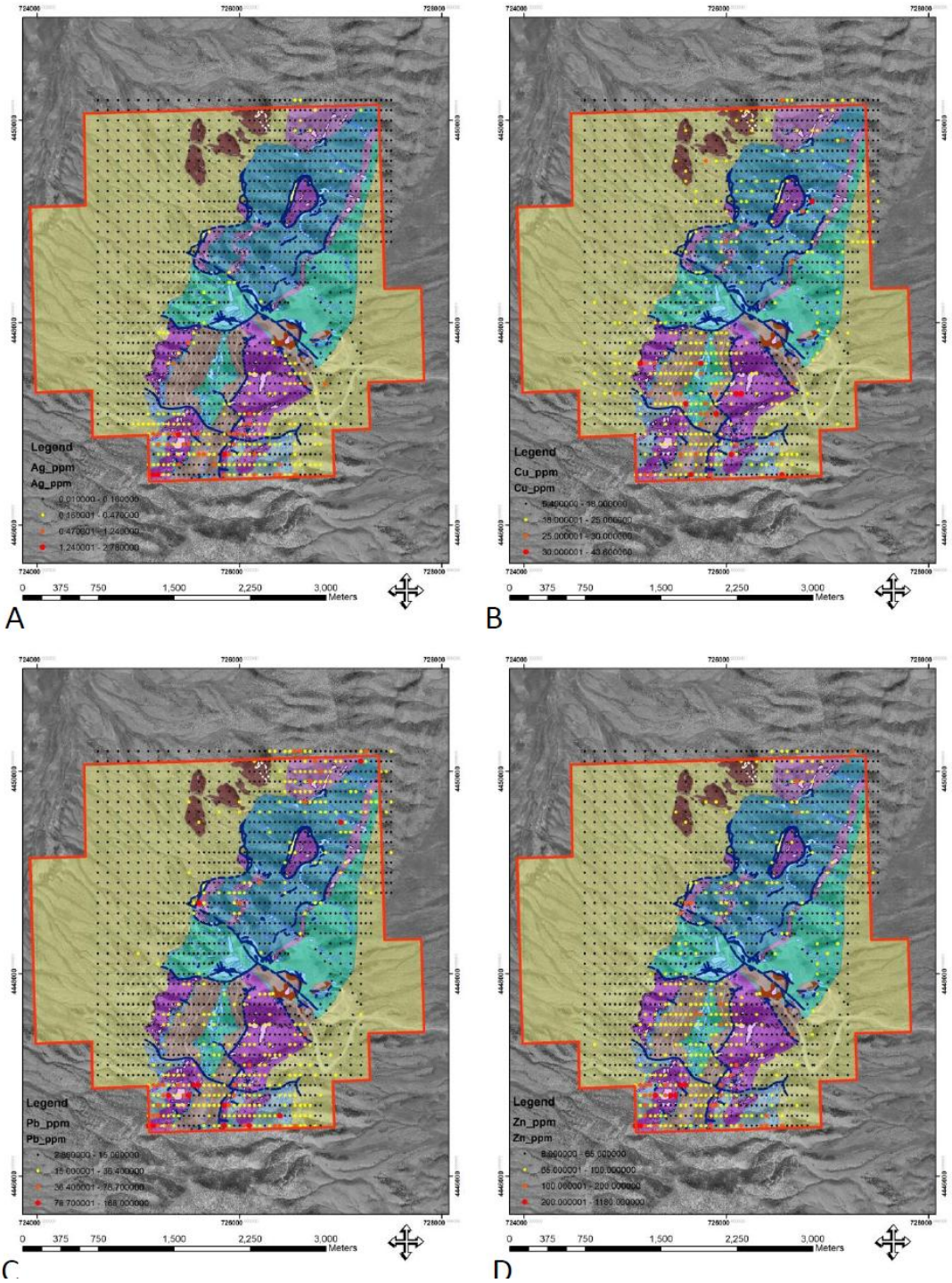

Figure 35. Geochemical maps illustrating south to north variability in Ag, Cu, Pb, and Zn content in the soil grid.

Discussion of Mineralization

Strata-bound mineralization with invisible gold occurs at the Candland Shale and Big Horse Limestone contact, although it can exist in any unit present. The most important factors that allow for strata-bound mineralization to occur are porosity and permeability. The two units that contain the most strata-bound mineralization are also finely bedded and sheared, both of which contribute to increased porosity and permeability. Alta gold, when exploring for additional gold mineralization, was confident that the Lamb Dolomite was the bottom of mineralization. This was based on their surface experience with the Candland Shale and Big Horse Limestone acting as the most favorable strata-bound host. This resulted in incomplete mapping of the claim, as well as stopping all drilling at an average of only 200 ft. Geologic mapping has determined that a maximum of 50 m of limestone is exposed at the surface below the Lamb Dolomite, although a much larger surface area exists (figure 18).

Gold mineralization associated with jasperoid development is structurally hosted. Two orientations of structures commonly host jasperoid, northwest-trending, high-angle structures and the low-angle Snake Fault (figure 3). Barren jasperoid occurrences far outnumber those containing detectable gold concentrations. The intensity of jasperoid replacement varies by proximity to the structures involved, displaying a gradation from quartz veining to stockwork veining to quartz flooding and full-scale jasperoid development.

Another type of silicification occurs by the replacement of stratigraphy. Cave-fill breccias, now wholly silicified, typify this event. In a similar manner, the Big Horse limestone is silicified for a strike length in excess of one kilometer, with gold mineralization increasing as the mined strip is approached.

The following is a brief summary of the style of mineralization as observed in the pits, as well as derived from reports by previous exploration geologists. As shown in figure

4, a total of seven individual deposits have been mined. These deposits change characteristics depending on the stratigraphy present and proximity to structures.

The Main, Access, and Emancipation pits are hosted in Candland Shale below a faulted upper contact with the Notch Peak limestone. Disseminated mineralization parallels bedding and low-angle shears. A review of historic drilling data shows that mineralization is vertically zoned in these pits with a high-grade core that contains the majority of the gold. Lower grade mineralization envelops the core and eventually grades into non-economic concentrations.

In the Upper and Ridge pits mineralization is hosted in the upper Orr and lower Notch Peak formations with intense decalcification. Caves filled with sedimentary breccia are the host to gold mineralization and contain cave material that is moderately to intensely silicified. Walking along the haul roads, these caves were sampled with gold values determined to be in excess of 0.5 ppm. The now partially filled Upper Main pit represents the transition between the two hosts with both cave-fill and bedding-replacement mineralization being present.

It is proposed that gold mineralization was driven by an intrusive heat engine, possibly, but not necessarily the exposed quartz monzonite porphyry to the south. All of the above mentioned northeast-oriented features (bedding, faults, and fold hinges) served as ground preparation and existed at the time of the quartz monzonite intrusion and gold-mineralizing event. Fluids traveled away from the heat source, either laterally or vertically along these pathways, especially along the contacts, until they intersected the northwest-trending structure that represents the mined strip (figure 36). Fluids were able to travel with minimal interaction with the carbonates until an unknown change in conditions, caused mineral deposition. The change could have been a temperature difference, pressure difference, chemical difference (such as the present of iron), or some other unknown variable. One idea put forth by Christensen and MacFarlane (2010) was that if karsting

occurred, it may have concentrated iron within the cave-fill materials, which were in turn later sulfidized by the mineralizing fluids. The best developed caves occur along northwest-trending structures, with the largest of these being the mined strip, which in this model would have acted as the main fluid pathway (figure 36). While fluids penetrated the Orr Formation, gold was disseminated along bedding planes and structures, while in the overlying limestones, cave-fill material was the receptive rock type.

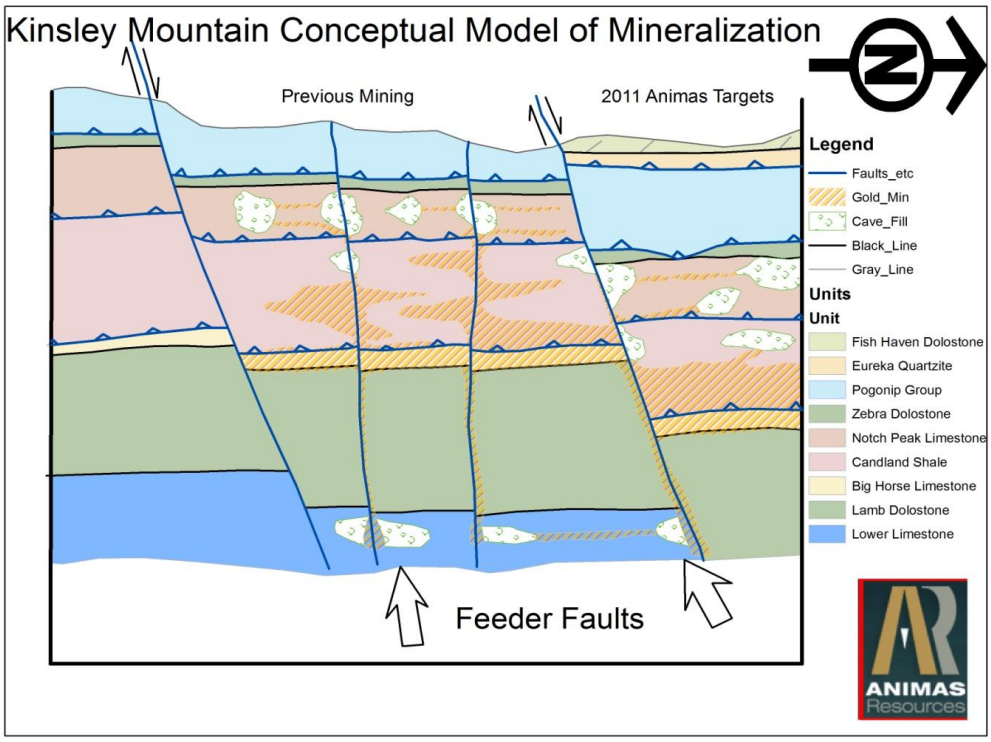

Figure 36. Conceptual model section of gold mineralization across the mined strip.

To test the intrusive-driven model for mineralization, the spatial distribution of other elements associated with Au mineralization were analyzed in ArcGIS. The multi-element data set was also analyzed by statistical methods to look for correlations and pathfinder elements. The details of this study are presented below, but the most important factor to come out of this was a strong positive correlation between Au and Te (0.81 correlation coefficient) in the soil dataset. This correlation, in combination with weaker associations to base metals further substantiates the igneous model. In the stream-sediment

dataset, the strongest correlation with Au is Bi, also potentially indicative of a skarn-related source (Barnes, 1979).

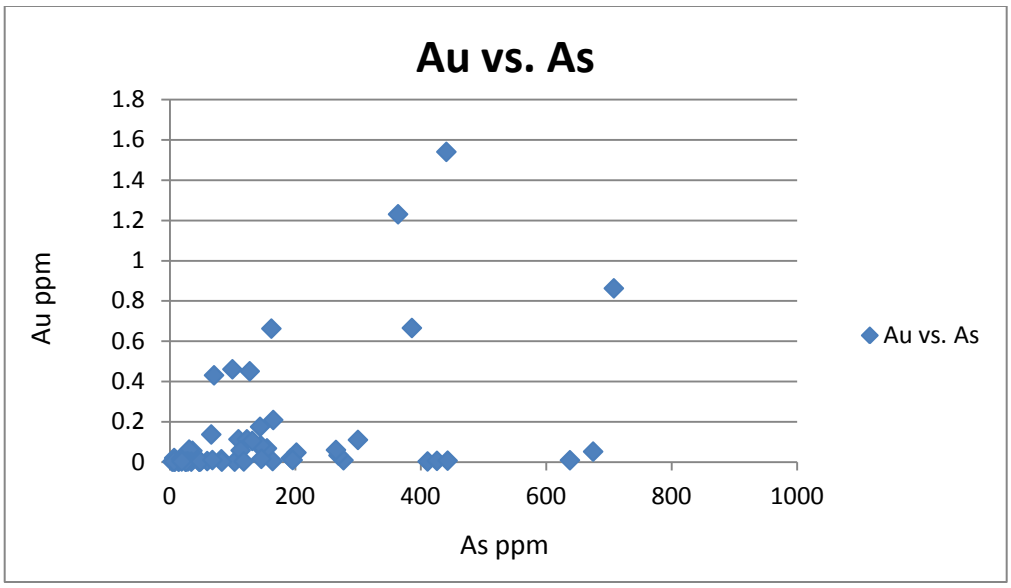

Figure 37. Plot of gold versus arsenic from rock chip data set.

The plot in figure 37 shows gold versus arsenic in the rock chip data set from Kinsley Mountain. The blue diamonds in figure 37 represent samples, with gold values reported in ppm. By comparing is plot with those generated by Arehart et. al. (1993), it appears that gold and arsenic display some positive correlation. When a similar plot of the soil data is constructured, it shows scatter and can not be used to evaulate a positive correlation. The reason a positive correlation is significant is that gold in Carlin-type systems is generally positively correlated to arsenic, as the two are involved in coupled substitution within the pyrite crystal structure (Arehart et. al., 1993).

Mineralization Conclusion

Although differing in morphology, from the perspective of gold, the styles of gold mineralization are genetically all related to an intrusion-driven system. The gold mineralization is not directly associated with the margins of the causative intrusion, but rather is distal disseminated most commonly occurring in structurally prepared host rock.

The causative intrusion may be the exposed quartz monzonite located at the south of the range, although it may also be a deeper seated, unexposed intrusion below the mined strip. If the hypothetical intrusion below the mined strip exists, it could be analogous to the 39 Ma Ibapah pluton of the Deep Creek Range, which intrudes into a northwest-trending accommodation structure (Ponce and Sampson, 1994). This conclusion about and intrusive relationship is primarily based on the geochemical associations found in all datasets. These include the association with tellurium and arsenic in soils, bismuth in stream sediments, and chlorite and epidote in hand samples. If the observation and interpretation, made by John Wilson (2010, pers. comm..) during a field visit, that a potential breccia pipe with mineralization is present in the Lower Main pit, it would further substantiate the interpreted intrusion related style of gold emplacement.

From this study, it has been concluded that gold transport at Kinsley Mountain was not associated with sulfidation. This was due to the overall lack of correlation between gold and sulfur and more importantly the lack of correlation as the Au grade increased. The process of coupled substitution of gold and arsenic in auriferous pyrite may have played a role in gold deposition as suggested by the rock-chip data set (figure 37). The soil data set, on the other hand, is to busy to either support or refute the association of gold and arsenic coupled substitutions. Within the literature, the method that is best utilized for determination of chloride vs. bisulfide complexing are fluid inclusion studies. Without such data, a more qualitative asessment of the overall metal zonation was used to suggest a temperature dependance to the deposition (figure 35). Although both chloride and bisulfide complexing are impacted by changes in temperature with the resulting precipitation of metal-bearing minerals, the chloride complexing may be more susceptible to these changes and is thought to have played the most important role in transporting metals at Kinsley Mountain.

Mineralization at Kinsley Mountain may be distally disseminated from an igneous source. It is not clear if the responsible intrusion is the exposed quartz monzonite to the

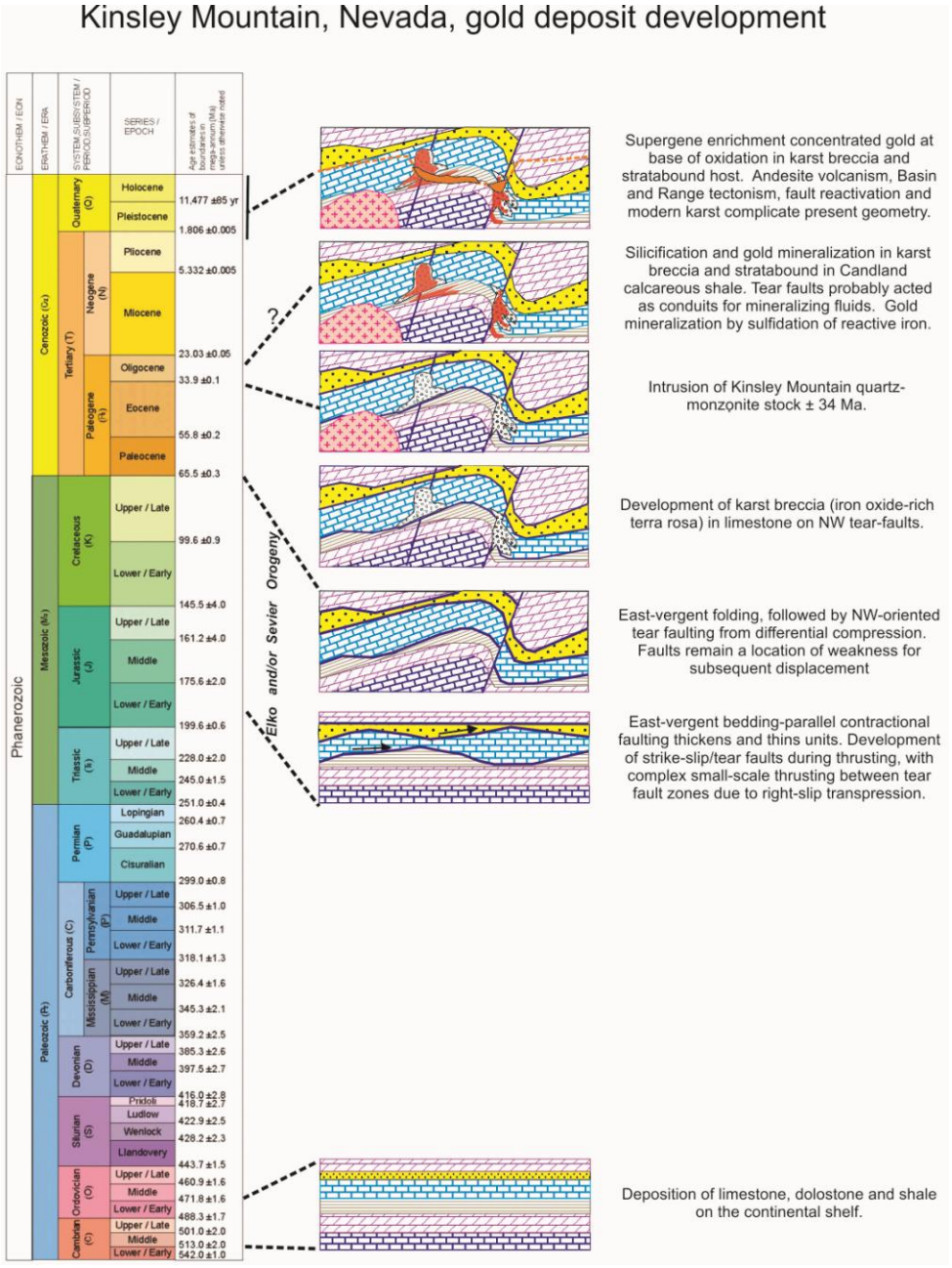

Figure 38. Events that bracket silicification associated with gold mineralization. (Christensen and MacFarlane, 2010)

south or another igneous body that is not exposed at the surface, potentially at depth below the mined strip. Although bedding-parallel mineralization occurs in the Candland Shale, the presence of silicified cave-fill breccia and second order northeast trends to mineralization, suggest channeling of fluids along pre-existing structural fabrics and bedding until the northwest-trending structures were encountered.

Chapter 5

CONCLUSIONS AND FINDINGS

The stratigraphic section (Figures 10, 11, 12) at Kinsley Mountain is more similar to stratigraphic sections in Utah than mountain ranges further west in Nevada (Figure 13), it follows that the units should be called by the same nomenclature. By associating the stratigraphic package at Kinsley with that of western Utah rather than east-central Nevada, a prediction for unexposed rocks below the lower limestone has been put forth. This has important implications for further exploration programs as the depth of potentially favorable host rock has been extended in an area that has not been drilled deeper than a couple of hundred meters.

If the age determination of the quartz monzonite is accurate at 34 Ma and it is overlain by andesitic volcanic rocks that are roughly the same age, then it follows that the quartz monzonite was uplifted and exposed within a very short interval of time, on the order of a couple million years. Steininger (pers. comm., 2010) characterized the texture of the quartz monzonite to indicate deep cooling of the intrusion as the crystals are moderately large. Although none was observed in the field, a large normal fault could be present between the two units. Alternatively the quartz monzonite could be the intrusive phase of the andesitic volcanics, with phenocrysts being slightly older than the aphanitic groundmass. A third possibility is that the age determination in the stock was actually gathered from a post-intrusion dike. The Jurassic quartz monzonite in the Goshute Range is visually similar to the stock at Kinsley Mountain.

A structural history for Kinsley Mountain has been determined including a progressive compressional event followed by an equally impressive progressive extensional episode that is ongoing. The mined strip had two stages of movement, potentially setting constraints on the age of gold mineralization. If the thrust fault and F1 folds are both offset along the northwest-trending shear, this places a maximum age constraint on the origination

of the Mined Strip accommodation structure. Since cave fill material along this structure is preferentially silicified and mineralized, as is the low-angle Snake Fault, a lower bracket on the mineralization is established. The latest movement along the Strip Fault, with resulting cave formation has mineralized fragments in the breccia, which requires a reactivation of the Strip Fault.

Through the use of correlation coefficients and factor analysis, a minimum of two pulses of metal enrichment are proposed to have occurred at Kinsley Mountain. The time gap between these pulses is unknown and could range from tens of years to millions of years. The earlier pulse is a base-metal-rich system, likely associated with the exposed quartz monzonite intrusion to the south, which has visible sulfide mineralization. The second pulse of mineralization was responsible for the gold emplacement. Although the time gap between pulses could be very narrow, correlations coefficients and factor scores argue for separate time for metal deposition. Furthermore, rock-chip sampling of visible base-metal mineralization contained no anomalous gold. Coarse calcite crystals are cut by a stage of quartz veining, potentially related to hydrothermal fluids associated with Tertiary normal faulting. More sulfide and arsenic were associated with mineralization than is evident from the pit walls, as observed by walking the dumps. The 0.40 correlation between gold and arsenic could be partially explained by biased sampling of oxide material that was collected at the surface.

Using geochemical associations to gold, it is proposed that gold mineralization is distally disseminated from an intrusive source. The strong correlation with tellurium in the soil data set in combination with the weaker correlations to tungsten, thallium, and molybdenum indicate the intrusion may be felsic. The correlation with gold and bismuth in stream sediment samples may indicate gold-bearing skarn, also related to an intrusion. Finally, the interpretation by John Wilson (2010, pers. comm.) and the author that a breccia

observed in the Lower Main pit is actually a breccia pipe, lead the author to call upon an intrusion related driver to the gold mineralization process.

By utilizing the material that makes up cave fill breccias along the mined strip and other parallel northwest-trending faults, multiple movements along the strip structures have been shown. This is a significant finding as these movements bracket the main stage gold mineralizing event, as mineralized fragments have been observed in the younger generation of cave fill material. Although the bracket does not have absolute timing, the younger generation of cave fill is associated with a generation of fault movement that post-dates the emplacement of the 34 Ma dike, thus necessitating that mineralization is contemporaneous with or older than 34 Ma, but younger than the host northwest structure, likely an accommodation structure originally developed in the Mesozoic.

REFERENCES

Allmendinger, R., 2006, Stereonet v. 1.2.0 software, http://www.geo.cornell.edu/geology/faculty/RWA/programs.html.

Alta Gold, 1994. Kinsley Gold Property Project Overview, Alta Gold internal report, p. 51.

Arehart, G.B., Chryssoulis S.L., and Kesler, S.E., 1993. Gold and Arsenic in Iron Sulfides from Sediment-Hosted Disseminated Gold Deposits: Implications for Depositional Processes. Economic Geology, v.88, pp. 171-185.

Barnes, H.L., 1979. Solubilities of ore minerals. In Barnes, H.L., eds., Geochemistry of hydrothermal ore deposits, pp. 404-460.

Buckley, C.P., 1967. Structure and stratigraphy of the Kinsley Mountains, Elko and White Pine Counties, Nevada, unpublished M.S. thesis, San Jose State University, San Jose, California, 50 p.

Christensen, O.D., and MacFarlane, B.J., 2010. Kinsley Mountain Project Elko County, Nevada, 2010 Annual Exploration Report *report for* Animas Resources Ltd., p49.

Christensen, O.D., 2010. Personal Communication – several field visits, technical discussions, presentations, and phone calls.

Coats, R.R., 1987, Geology of Elko County, Nevada: Nevada Bureau of Mines and Geology Bulletin 101, 112 p.

Cowdery, P.H., 2003. A Technical Report on the Kinsley Mountain Gold Project, *report for* LaTeegra Resources Corporation, p. 27.

Cowdery, P.H., 2007. A 43-101 compliant Technical Report for the Kinsley Mountain Gold Project, *report for* Intor Resources Corporation a subsidiary of Nevada Sunrise LLC, p. 42.

Crafford, A.E.J., 2007. Geologic Map of Nevada: U.S. Geological Survey Data Series 249, 1 CD-ROM, p. 46, 1 plate.

DeCelles, P.G., 2004. Late Jurassic to Eocene evolution of the Cordilleran thrust belt and foreland basin system, western U.S.A: American Journal of Science, v. 304, p. 105–168.

Desilets, M.O., 1992. Ion pedogeochemistry of the Kinsley Mountains deposit, Nevada, M.S. thesis, University of Nevada, Reno, 76 p.

Dohrenwend, J.C., Schell, B.A., and Moring, B.C., 1991, Reconnaissance photogeologic map of young faults in the Elko 1° by 2° quadrangle, Nevada and Utah: U.S. Geological Survey Miscellaneous Field Studies Map MF-2179, 1 sheet, scale 1:250,000.

DuBray, E.A., 2007. Time, space, and composition relations among northern Nevada intrusive rocks and their metallogenic implications, Geosphere, v. 3, no. 5, p. 381-405.

Dunham, 1955. Geology and Geophysical Survey of Morning Star Mine and Dotty Mine, Boone Springs, White Pine County, Nevada, p. 17.

Gans, P.B., Miller, E.L., Houseman, G., and Lister, G.S., 1991, Assessing the amount, rate, and timing of tilting in normal fault blocks: a case study of tilted granites in the Kern-Deep Creek Mountains, Utah: Geological Society of America Abstracts with Programs, v. 23, no. 2, p. 28.

Hintze, L. F., 1988, Geologic history of Utah: Brigham Young University Geology Studies Special Publication 7, 202 p.

Hose, R.K., Blake, M.C., and Smith, R.M., 1976. Geology and Mineral Resources of White Pine County, Nevada. Nevada Bureau of Mines and Geology, Bulletin 85, p. 105.

Howard, K.A., 2003. Crustal Structure in the Elko-Carlin Region, Nevada, during Eocene Gold Mineralization: Ruby-East Humboldt Metamorphic Core Complex as a Guide to the Deep Crust, Economic Geology, Vol. 98, pp. 249-268.

Ketner, K.B., Day, W.C., Elrick, M., Vaag, M.K., Zimmermann, R.A., Snee, L.W., Saltus, R.W., Repetski, J.E., Wardlaw, B.R., Taylor, M.E., Harris, A., 1998. An outline of tectonic, igneous, and metamorphic events in the Goshute-Toano range between Silver Zone pass and White Horse pass, Elko county, Nevada: a history of superposed contractional and extensional deformation. U.S. Geological Survey Professional Paper 1593, 1–12.

LaPointe, D.D., Tingley, J.V., and Jones, R.B, 1991. Mineral Resources of Elko County, Nevada: Nevada Bureau of Mines and Geology, Bulletin 106, 236 p.

Lee, F., 2004. Report on the Clifton-Gold Hill Property Gold Hill Mining District, Tooele County, Utah, U.S.A., *report for* Dumont Nickel, Inc., p. 101.

Lush, A.P., McGrew, A.J., Snoke, A.W., and Wright, J.E., 1988. Allochthonous Archean basement in the northern East Humboldt Range, Nevada. Geology, v. 16, no. 4, p.349-353.

MacFarlane, B.J. 2010. Kinsley Mountain Project Elko County, Nevada, 2010 Exploration Summary Report *report for* Animas Resources Ltd., p. 57.

Marshak, S., and Mitra, G. 1988. Basic Methods of Structural Geology. Prentice Hall, p.446.

Maldonado, F., Spengler, R.W., Hanna, W.F., and Dixon, G.L., 1988, Index of granitic masses in the state of Nevada: U.S. Geological Survey Bulletin 1831, 81 p.

Miller, D.M., Hillhouse, W.C., Zartman, R.E., and Lanphere, M.A., 1987. Geochronology of intrusive and metamorphic rocks in the Pilot Range, Utah and Nevada, and comparison with regional patterns. Geological Society of America Bulletin, v. 99, p. 866-879.

Miller, E.L., and Gans, P.B., 1989. Cretaceous crustal structure and metamorphism in the hinterland of the Sevier Thrust belt, Western U.S. Cordillera. Geology, v. 17, p. 59-62.

Miller, E.L., Dumitru, T.A., Brown, R.W., and Gans, P.B., 1999. Rapid Miocene slip on the Snake Range-Deep Creek Range fault system, east-central Nevada. *GSA Bulletin*; June 1999; v. 111; no. 6; pp. 886–905.

Monroe, S.C., Suda, R.U., Wobzicki, W.A., Suda, C.E., and Langen, E.B., 1988. Kinsley Mountain Project Exploration Report, Cominco American Resources Incorporated internal document, p. 57.

Monroe, S.C., 1990. Kinsley Mountain project, Elko County, Nevada, *in* Shaddrick, D.R., Kizis, J.A., and Hunsaker, E.L., editors, Geology and Ore Deposits of the Northeastern Greatt Basin, Field Guide for Field Trip No 5, Great Basin Symposium, Geological Society of Nevada, pp. 170-183.

Muntean, J.L., Cline, J.S., Simon, A.C., and Longo, A.A., 2011. Magmatic-hydrothermal origin of Nevada's Carlin-type gold deposits. Nature Geosciences, v. 4, pp. 122-127.

Muntean, J., Tarnocal, C., Coward, M., Rouby, D., and Jackson, A., 2001, Styles and restorations of Tertiary extension in north-central Nevada, *in* Shaddrick, D.R., Zbinden, E., Mathewson, D.C., and Prenn, C., editors, Regional tectonics and structural control of ore: the major gold trends of northern Nevada, Geological Society of Nevada Special Publication 33, p. 55–69.

Nelson, S.T., Hart, G.L., and Frost, C.D., 2011. A reassessment of Mojavia and a new Cheyenne Belt alignment in the Eastern Great Basin. Geosphere, v. 7, no. 2, p. 513-527.

Nutt, C.J., and Thorman, C.H., 1994, Geologic map of the Weaver Canyon quadrangle, Nevada and Utah, and parts of the Ibapah Peak quadrangle, Utah, and Tippett Canyon quadrangle, Nevada: U.S. Geological Survey Open-File Report 96-635, scale 1:24,000

Paige, R.A., and Hanlund, W.M., 1962. Geologic Map of the Southern Kinsley Mountains. 1 plate.

Perry, K., 2010. Detrital zircon geochronology for Neoproterozoic to Cambrian sediment sources of the Deep Creek Range and the Pilot Range in the Southwestern United States. Senior Project, California Polytechnic State University, San Luis Obispo, CA., p. 40.

Piekenbrock, J., 2009. Personal communication – Santa Gertrudis Mine - lecture/short course on factor analysis.

Ponce, D.A., and Sampson, J.A., 1994. Basin Geometry of the Goshute Indian Reservation, Eastern Nevada and Western Utah *in* Thorman, C.H., Nutt, C.J., and Potter, C.J., eds., 1994, Dating of Pre-Tertiary attenuation structures in Upper Paleozoic and Mesozoic Rocks and the Eocene history in northeast Nevada and northwest Utah: Nevada Petroleum Society, Sixth Annual Fieldtrip Guidebook, p. 126.

Premo, W.R., Castineiras, P., and Wooden, J.L., 2008. SHRIMP-RG U-Pb isotopic systematic of zircon from the Angel Lake orthogneiss, East Humboldt Range, Nevada: Is this really Archean crust?; Geosphere, v. 4, p. 963-975.

Quigley, W.D., 1966. Developmental Program for Kinsley Marble Deposit. *Report for* Western Marble Company, Ltd., p.19.

Rahl J.M., McGrew, A.J., and Foland, K.A., 2002. Transition from Contaction to Extension in the Northeastern Basin and Range: New Evidence from the Copper Mountains, Nevada, *The Journal of Geology*, Vol. 110, No. 2, pp. 179-194.

Robinson, J.P., 2005. The Kinsley mine – A structure-controlled sediment-hosted disseminated gold deposit in eastern Nevada, *in* Rhoden, H.N., Steininger, R.C., and Vikre, P.G., eds., Geological Society of Nevada Symposium 2005: Window to the World, Reno, Nevada, May 2005, p. 469-481.

Rodgers, D.W., 1987, Thermal and structural evolution of the southern Deep Creek Range, west central Utah and east central Nevada: Palo Alto, California, Stanford University, Ph.D. dissertation, 149p.

Santos, J., 2007. Kinsley Mountain Project Calloway Geologic Interpretation for Nevada Sunrise LLC.

Satarugsa, P., and Johnson, R.A., 2000. Cenozoic tectonic evolution of the Ruby Mountains metamorphic core complex and adjacent valleys, northeastern Nevada, *Rocky Mountain Geology*, v. 35, no. 2, pp. 205-230.

Silberling, N.J., Nichols, K.M., Trexler Jr., J.H., Jewell, P.W., and Crosbie, R.A., 1997. Overview of Mississippian Depositional and Paleotectonic History of the Antler Foreland, Eastern Nevada and Western Utah. In: Link, P.K., and Kowalis, B.J. (Eds.), Geological Society of America Field Trip Guidebook, BYU Geological Study 42 (1), pp. 161-196.

Silberling, N.J., Nichols, K.M., 2002. Structural evolution of the White Horse pass area. Nevada Bureau of Mines and Geology Map 132 (1), 24000.

Silberling, N.J., Nichols, K.M., 2002. Structural evolution of the White Horse pass area. Text and References to accompany Nevada Bureau of Mines and Geology Map 132, p. 8.

Sillitoe, R.H., and Bonham, H.F., 1990. Sediment-hosted gold deposits: Distal products of magmatic-hydrothermal systems. Geology, v. 18, p. 157-161.

Steininger, R., 1966, Geology of the Kinsley mining district, Elko County, Nevada: Brigham Young University Geology Studies, v. 13, p. 69–88.

Steininger, R., 2010. Personal communication – field visit.

Teal, L. and Jackson, M., 2002. Geologic overview of the Carlin Trend gold deposits, *in* Thompson, T.B., Teal, L., and Meenwig, R.O., (Eds.). Gold deposits of the Carlin Trend, Nevada Bureau of Mines and Geology, Bulletin, 111. Pp. 9-19.

Thorman, C.H., and Peterson, F., 2004. The Middle Jurassic Elko orogeny – A major tectonic event in Nevada-Utah. Search and Discovery Article #30022. Adapted from "extended abstract" for AAPG Annual Meeting, Salt Lake City, Utah, May 11-14, 2003. p.7.

Thorman, C.H., August 16, 2010. Chuck Thorman Kinsley Report, Animas Resources internal document, p. 7.

Thorman, C.H., 2010. Personal communication – Kinsley Mountain field visit, lecture, field trip.

Wannamaker, P.E., and Doerner, W.M., 2002. Crustal structure of the Ruby Mountains and southern Carlin region, Nevada, from magnetotelluric data, *Ore Geology Reviews*, v.21, pp. 185-210.

Welsh, J.E., 1994. Middle Jurassic tectonic plates: Ferguson Mountain, Elko County, Nevada *in* Thorman, C.H., Nutt, C.J., and Potter, C.J., eds., 1994, Dating of Pre-Tertiary attenuation structures in Upper Paleozoic and Mesozoic Rocks and the Eocene history in northeast Nevada and northwest Utah: Nevada Petroleum Society, Sixth Annual Fieldtrip Guidebook, p. 126.

Wilson, M.L., and Dennis, R.D., 2006. Western Cordillera, an Intergrated Petroleum Evaluation of Northeastern Nevada, http://westerncordillera.com/mesozoic()_folding.htm.

Wilson, J.R., 2010. Personal communication – field visit, technical discussion.

Zamudio, J.A., and Atkinson, W.W., Jr., 1992. Mesozoic deformation in the Dolly Varden Mountains and Currie Hills, Nevada: Geological Society of America.